IACMI/R010-2022/7.3

Project 7.3 Characterization of Kevlar®-Reinforced Composites for Predictive Simulation

Author: Jennifer Galvin
Date: May 10, 2022

Final Technical Report
PA16-0349-7.3-01

Approved for Public Release.
Distribution is Unlimited.

The Institute for iacmi Advanced Composites Manufacturing Innovation
THE COMPOSITES INSTITUTE

U.S. DEPARTMENT OF ENERGY

The information, data, or work presented herein was funded in part by the Office of Energy Efficiency and Renewable Energy (EERE), U.S. Department of Energy, under Award DE-EE0006926

Authors acknowledge the contributions of Karl Chang, DuPont, to this work.

Characterization of Kevlar®-reinforced Composites for Predictive Simulation

Principal Investigator: Jennifer Galvin

Organization: The DuPont Company

Address: 5401 Jefferson Davis Highway, Richmond, VA 23234

Phone:

Email: Jennifer.m.galvin@dupont.com

Co-authors: Jennifer Galvin, Rebecca Cutting, Alex Reichanadter, Jan-Anders Mansson, Johnathan Goodsell

Date Published: (May, 2022)

Prepared by:
Institute for Advanced Composites Manufacturing Innovation
Knoxville, TN 37932
Managed by Collaborative Composite Solutions, Inc.
For the
U.S. DEPARTMENT OF ENERGY
Under contract DE- EE0006926

Project Period:
(08/2018 – 12/2020)

Approved for Public Release

TABLE OF CONTENTS

LISTS

LIST OF ACRONYMS

DIC	Digital image correlation
FPM	Feet per minute
g	grams
GPa	Giga Pascals
Hz	Hertz
in	inches
IR	Infrared
MDLab	Manufacturing Design Laboratory
mm	millimeters
Mpa	Mega Pascals
PEEK	Polyether ether ketone
psi	pounds per square inch
RPM	Revolutions per minute
Std Dev	Standard Deviation

List of Figures

List of Tables

List of Appendices

7.3 Project Introduction

The IACMI 7.3 project between DuPont and Purdue University was focused on initial material characterization of Kevlar® fiber for automotive applications. As carbon fiber composites can delaminate and fragment in the event of an automobile crash, it is expected that a Kevlar-carbon hybrid might offer improved crash performance. However, to design a hybrid composite structure, the designer will need modeling and simulation tools, and these require material property input values. Hence, this initial exploration into Kevlar for automotive applications focused on developing a preliminary set of material properties essential for both manufacturing and performance simulation, with the intent to provide DuPont with the technical information to determine feasibility of further development.

Two material systems were characterized. The first is a Kevlar®,[1] 49, 2x2 twill weave with Hexion EPIKOTE resin provided by a commercial pre-pregger. The second is a unidirectional Kevlar®/VZL-36D (polyamide-based) prepreg tape manufactured at Purdue University. In addition to the characterization data, the thermoplastic tape (TP) manufacturing experience may prove valuable to DuPont in evaluating future material options. These two data sets provide a technical base from which DuPont can develop technical strategy for further evaluation and development of Kevlar® for automotive applications.

Headings in this report correspond to project task numbering, apart from the concluding sections. Subtask 7.3.1 was project management. Subtask 7.3.2 was characterization of dry Kevlar material and resins. Because Hexion could not supply raw EPIKOTE resin in experimental quantities, and because the project was already over budget and behind schedule, it was decided to omit Subtask 7.3.2. This decision was communicated by the project team to IACMI HQ on a monthly project review call. The technical data sheets provided by the resin vendor (available at time of report preparation) do provide working times and characteristics for the "in process' resin and also for mechanical properties of the cured resin system.

[1] Kevlar® is a registered trademark of DuPont de Nemours, Inc

Subtask 7.3.3 Kevlar®/Epoxy Prepreg Characterization

Executive Summary

The IACMI 7.3 project between DuPont and Purdue University required the mechanical testing of a 2x2 twill Kevlar® weave with Hexion EPIKOTE resin. The tension, shear, flexure, and compressive behavior of this material system was characterized, and the results can be seen in Table 1. These material properties can now be further evaluated for use in performance simulations of automotive components to represent the properties of composites based on woven materials containing Kevlar. This report will provide details regarding the effort required to arrive at these material properties.

Table 1: Tabulated material characterization data of Kevlar weave with Hexion EPIKOTE resin

Sample Type	Modulus [GPa]	Std. Dev [GPa]	Strength [MPa]	Std. Dev. [MPa]
Tension	35.8	3.7	539.0	42.6
Shear	5.67	0.42	107.8	15.7
Flexure, 76.8mm span	30.3	0.4		
Flexure, 32.2mm span	30.0	0.3	477.3	12.9
Compression	19.7	1.6	150.6	8.8

Introduction

Characterization of a thermoset prepreg weave of Kevlar fibers and Hexion EPIKOTE resin was completed at the Composites Manufacturing and Simulation Center at Purdue University as part of the IACMI 7.3 project. The elastic stiffness, shear stiffness, flexural stiffness, and compressive stiffness were all experimentally measured, as well as the corresponding strengths. As the commercially available resin system was designed to be used for short cure cycles associated with compression molding, the majority of test samples were made using a press and a flat plate mold. However, several laminates were made in the oven and the autoclave to compare the tensile responses of the material system from different manufacturing methods. Each of the manufacturing methods applied different pressures and temperatures over the curing cycle, leading to differences in the performance of the materials. This report will detail the manufacturing process, sample preparation, analysis method, and description of the characterization results for each of the test methods employed.

Background

In an effort to increase fuel economy in light-weight vehicles, the automotive industry has been using increasing amounts of composite materials. Carbon fiber and fiber glass composites have been studied extensively in automotive environments and are in frequent use for vehicle components. However, another common composite fiber, Kevlar, has not been studied to such an extent for these applications. Kevlar has underlying benefits for the automotive industry like ductile failure mechanisms and impact tolerance that have not been widely utilized. Before Kevlar-containing composites can be incorporated more broadly into the automotive industry they must be studied and the necessary material properties need to be quantified experimentally. Once additional material properties of Kevlar composites made from material systems of interest to the automotive industry are more widely known, they can be used evaluated for use in manufacturing and performance simulations by automotive manufacturers. The goal

of the IACMI 7.3 project was to characterize the material properties of a Kevlar prepreg weave with a Hexion EPIKOTE resin system for consideration of future use within performance simulations.

Specimen Preparation

Flat laminates of the Kevlar woven/epoxy prepreg substrate were manufactured to create characterization coupons for all of the test methods. Nine laminates were manufactured for the study: 5 using a 30-ton press, 3 using an oven, and 1 with an autoclave. Each of the laminates had dimensions of 254 mm x 254 mm (10 x 10 in). The number of layers for each laminate varied: 7 laminates had 6 plies, 1 laminate had 8 plies, and 1 laminate had 12 plies. The laminates manufactured with the oven and the autoclave were subjected to vacuum and a slow ramp in temperature to 180°C. For the compression molded samples, room temperature material was placed in a pre-heated tool before immediately being pressed at 600 psi. The laminates remained at pressure for 20 minutes before being removed from the press and demolded.

Table 2 lists the layups, test standard, number of laminates, and manufacturing method for the test samples. A single ply of fabric is labeled as (0/90) or as (± 45) (when the fabric was rotated 45°) within this naming convention. Fiber volume fractions for the final laminates in this section were not determined.

Table 2: Number of laminates and samples produced for each of the testing methods as well as manufacturing method and layup

Test Standard	Plate Name	# of Laminates	# of Samples	# of Plies	Manufacturing Method	Layup
Tensile ASTM D3039	T-P-#	3	26	6	Press	$[(0/90)]_6$
	T-A-#	1	8	6	Autoclave	$[(0/90)]_6$
	T-O6-#	2	16	6	Oven	$[(0/90)]_6$
	T-O12-#	1	8	12	Oven	$[(0/90)]_{12}$
Shear ASTM D3518	S-P-#	1	8	8	Press	$[(\pm 45)]_8$
Compression Modified ASTM D695	CF-P-#	0.5 (Shared plate with flexure coupons)	11	6	Press	$[(0/90)]_6$
Flexure ASTM D7264	CF-P-#	0.5 (Shared plate with compressi	10	6	Press	$[(0/90)]_6$

		on coupons)				

The samples were cut out using a waterjet. This technique was intentionally chosen over a surface grinder because Kevlar material tends to fray during cutting operations with saw blades. The samples used for shear testing and the comparative tensile testing were 25.4 mm (1 inch) in width, and had 50.8 mm (2 inch) fiber glass tabs epoxied to the ends, leaving a 152.4 mm (6 inch) gage section in the middle. The dimensions for the samples came from ASTM D3518 and ASTM D3039 respectively. The tensile samples used strictly for characterization were cut into a dog-bone shape with dimensions following ASTM D638-14, which can be seen in
Figure 1. The switch in sample shape was done to reduce the number of steps required for sample preparation as well as the preparation time. The compression and flexure tests both used rectangle samples lengths around 100 mm and widths of 12-13 mm. The dimensions for these samples came from a modified version of ASTM D695 used by Boeing and ASTM D7264, respectively.

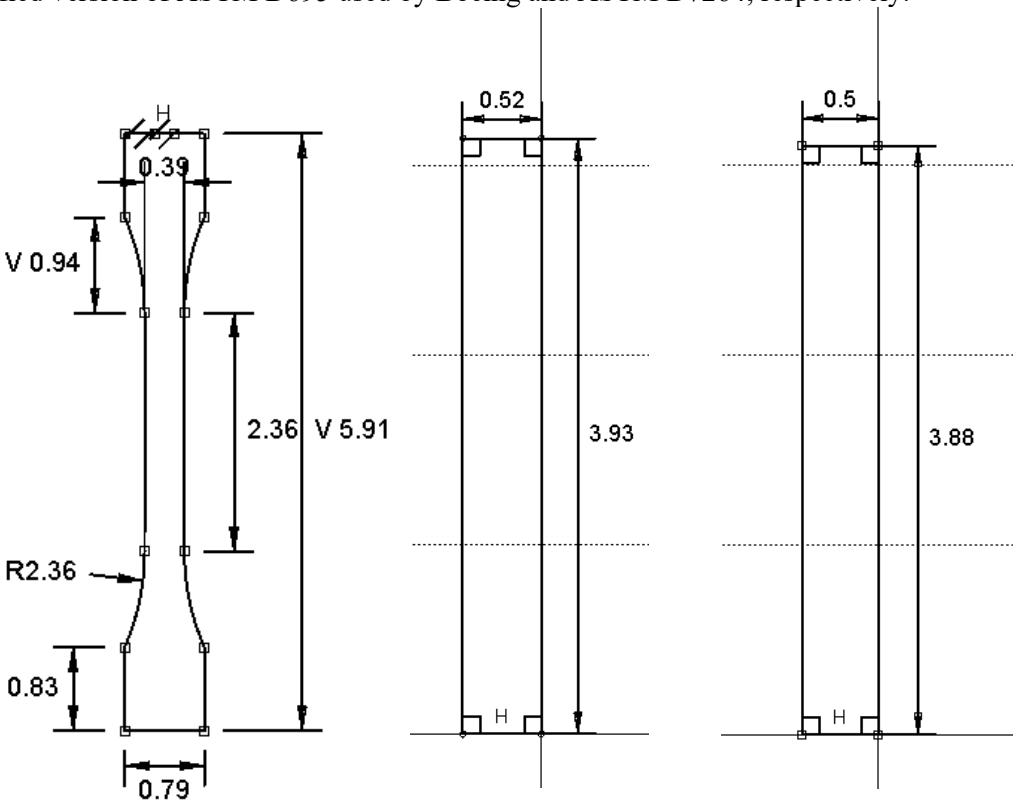

Figure 1: Dog-bone tensile (left), flexure (center), compression (right) sample dimensions in inches

Figure 2 and Figure 3 show tensile, compression, and flexure coupons after being cut by the waterjet but prior to being removed from the plate. Once the samples were extracted from the laminates, the tabs from the waterjet were ground off flattening the top and bottom surfaces of the samples. Because the samples were exposed to water during the preparation stage, an oven at low temperatures (~37°C) was used to dry out the samples prior to testing.

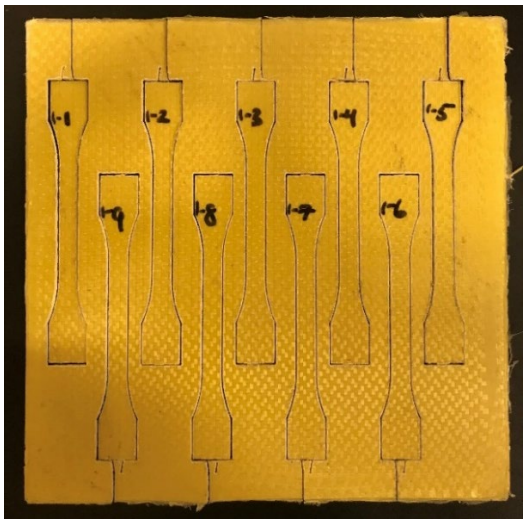

Figure 2: Dog-bone tensile samples after being cut by the waterjet with dimensions following ASTM D638-14

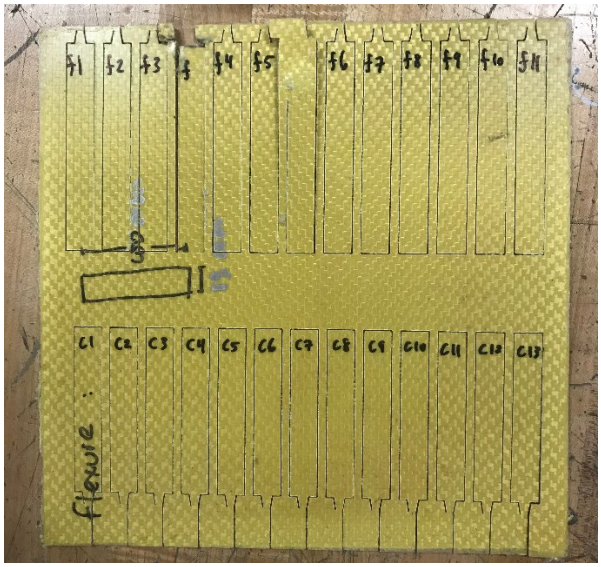

Figure 3: Flexure (top) and compression (bottom) samples after being cut by the waterjet with dimensions following ASTM D7264 and modified ASTM D695 respectively

The thickness and width were measured at 3 locations along the longitudinal axis of each sample. The average of these measurements was used in data reduction for each test. An MTS single axis load frame with a 22-kip load cell was used to test the tensile, shear, and compression samples while a different MTS single axis load frame with a 5-kip load cell was used to test the flexure samples.

Test Methodology

Tensile Testing

As previously stated, the tensile testing followed ASTM D3039. The crosshead movement on the MTS machine was set to a displacement rate of 2 mm/ min, and the load and displacement data were recorded at a rate of 10 Hz. The tensile samples were spray painted white and had a black speckle pattern applied to the gage section of the surface for digital image correlation (DIC) to be used. The DIC system allows for the calculation of the strain field on the surface of the sample by using images of the sample as it is

being loaded. The DIC took pictures of the sample at a 10 Hz rate as well. The samples were loaded until catastrophic failure occurred, and then data recording stopped, and the samples were removed from the MTS machine.

The load values from the MTS machine and the strain values from the DIC system were used to calculate the Young's modulus of the Kevlar woven composite as well as the tensile strength. The stress of the sample was defined as the load divided by the cross-sectional area, which in this case was the average width times the average thickness of the sample.

$$\sigma_t = \frac{P}{wt} \tag{1}$$

The stress was calculated for each datapoint recorded, allowing for a stress vs strain plot to be created. In addition, the strength of the sample was defined as the maximum stress the sample endured. The Young's modulus was defined as the slope of the stress-strain curve in the linear region of the curve.

$$E = \frac{\Delta\sigma}{\Delta\varepsilon} \tag{2}$$

Shear Testing

Shear testing was completed in a similar method to tensile testing, using ASTM D3518. This test standard uses $[\pm 45]_{ns}$ samples loaded in tension to determine shear modulus and strength. The samples were loaded in tension at a displacement rate of 2 mm/min and the load and displacement were recorded at a rate of 10 Hz. The DIC system was also used to calculate shear strain for the samples during testing.

The load and strain data were used to calculate the shear modulus and strength of the Kevlar weave. The shear stress of a $[\pm 45]_{ns}$ sample pulled in uniaxial tension is defined as the load divided by 2 times the average cross-sectional area. The shear strength is the maximum shear stress experienced by the sample during testing.

$$\tau_{12} = \frac{P}{2(wt)} \tag{3}$$

The shear modulus of elasticity is defined as the slope of the shear stress – shear strain curve.

$$G_{12} = \frac{\Delta\tau_{12}}{\Delta\gamma_{12}} \tag{4}$$

Compression Testing

Compression testing followed the modified ASTM D695 standard used by Boeing. A rectangular sample is prevented from buckling by being sandwiched between two flat metal laminates that are held together by 4 screws. The compressive load is introduced to the sample by a flat platen on the top cross head that contacts the top surface of the test sample sticking out above the two flat metal laminates, this can be seen in Figure 4. The top cross head was set to displace at a rate of 1 mm/min, and the load and displacement measurements were recorded at a rate of 10Hz. Testing was stopped once crushing or catastrophic damage was noticed. The primary surfaces of the sample are covered by the flat plat, which prevents the DIC from being used to obtain strain data.

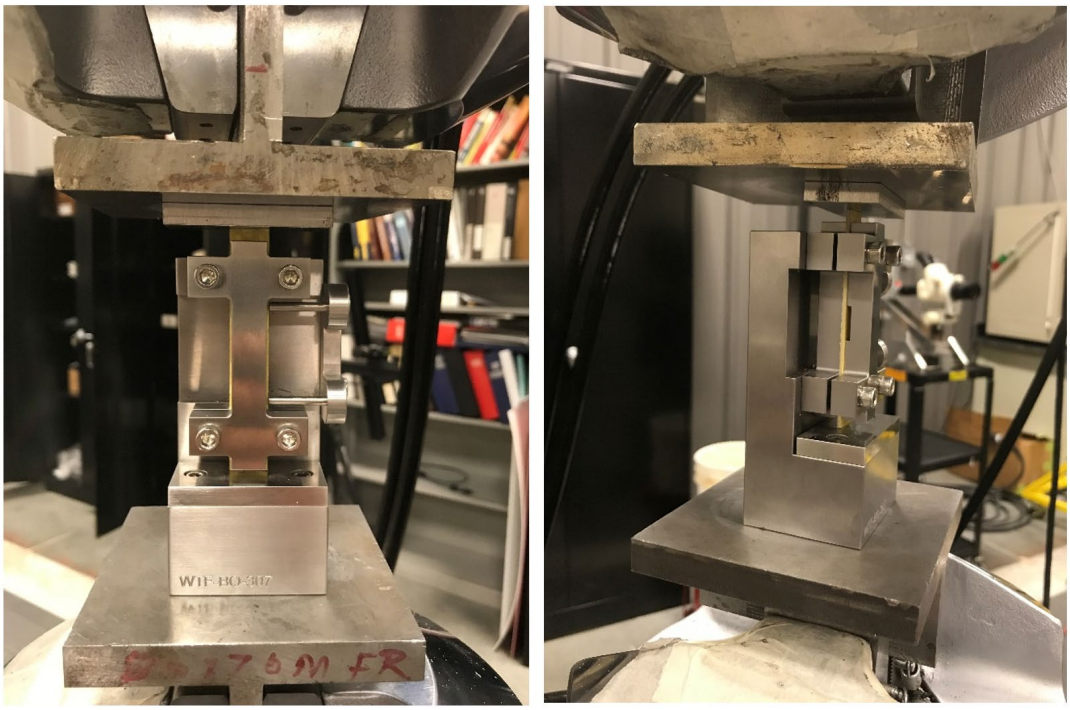

Figure 4: Compression test setup using the standard modified D695 test fixture

For the present preliminary study, instead of strain gauges, or digital image correlation, the strain of the sample was calculated using the following approximation

$$\varepsilon_c = \frac{\Delta L}{L} \tag{5}$$

The compressive stress of the sample was calculated using the same equation for tensile stress, force divided by the average cross-sectional area. The strength was defined as the maximum compressive stress experienced by the sample.

$$\sigma_c = \frac{P}{wt} \tag{6}$$

The compressive modulus was calculated as the slope of the linear portion of the stress-strain curve from the test.

$$E_c = \frac{\sigma_c}{\varepsilon_c} \tag{7}$$

Flexure Testing

Flexure testing, following ASTM D7264, was completed on the MTS machine with the 5-kip load cell. A 3-pt bend setup with a 76.8 mm span was used (see Figure 5), and the load was applied through the top pin located at the center of the span. The displacement rate was set to 1mm/min and the load and displacement measurements were recorded at 10 Hz.

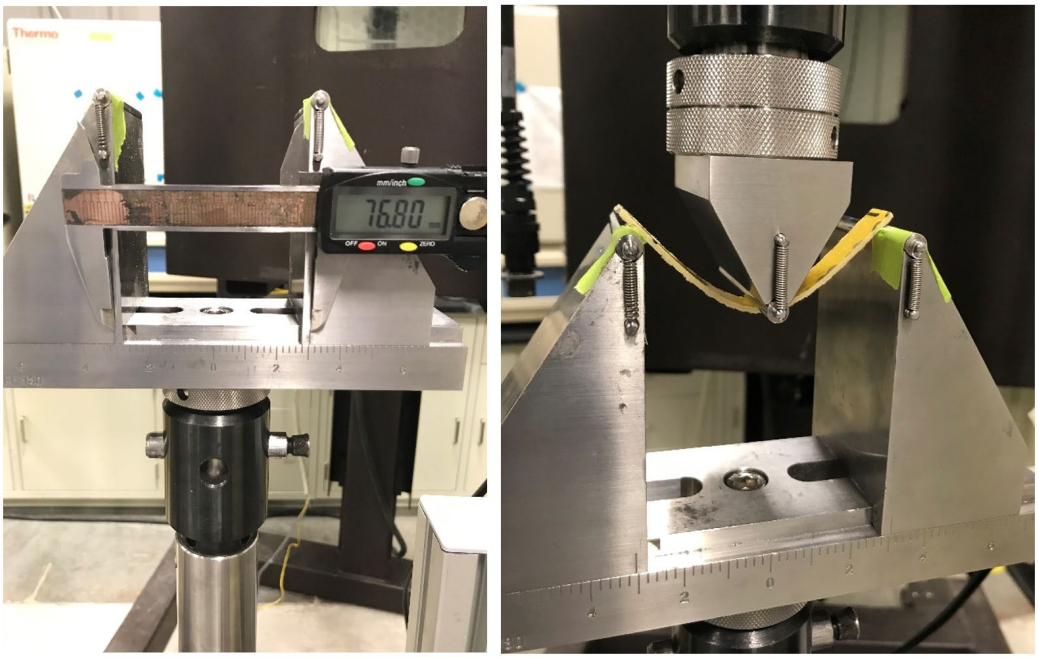

Figure 5: Flexure sample test setup using 3-point bending test fixture

Flexural stress is calculated using the load applied, the span, the average width, and thickness of the sample. The flexural strength is the maximum stress experienced by the sample during testing.

$$\sigma = \frac{3PL}{2wt^2} \tag{8}$$

The flexural stiffness of the weave can be calculated in 2 different ways. The first method is to use the slope of the load-displacement curve along with the span, width, and thickness of the sample

$$E_f = \frac{L^3}{4wt^3}\frac{\Delta P}{\Delta \delta} \tag{9}$$

The other option is to calculate the maximum strain of the sample at the outer surface of the mid-span using the displacement, span, and average thickness of the sample.

$$\varepsilon_f = \frac{6\delta t}{L^2} \tag{10}$$

Once the flexural strain is calculated, the flexural modulus can be calculated using the slope of the linear portion of the flexural stress vs flexural strain curve.

$$E_f = \frac{\Delta \sigma_f}{\Delta \varepsilon_f} \tag{11}$$

Results & Discussion

Tensile Samples

Two laminates of tensile samples, T-P-1 and T-P-2, were tested to failure and analyzed for stiffness and strength. Most of the dog-bone samples failed within the gage section (see Figure 6). Looking closer at the failed regions of the tensile coupons shows delamination between plies (see Figure 7). There was matrix failure as well as fiber failure in the test coupons. While the samples remain in one piece after testing, a slight pull on one end will completely separate the two pieces, revealing the weave is not still intact. The frayed ends of broken Kevlar fibers are also visible in the close-up view. This phenomenon was consistent across all of the tensile samples.

Figure 6: Failed tensile samples from laminates T-P-1 and T-P-2

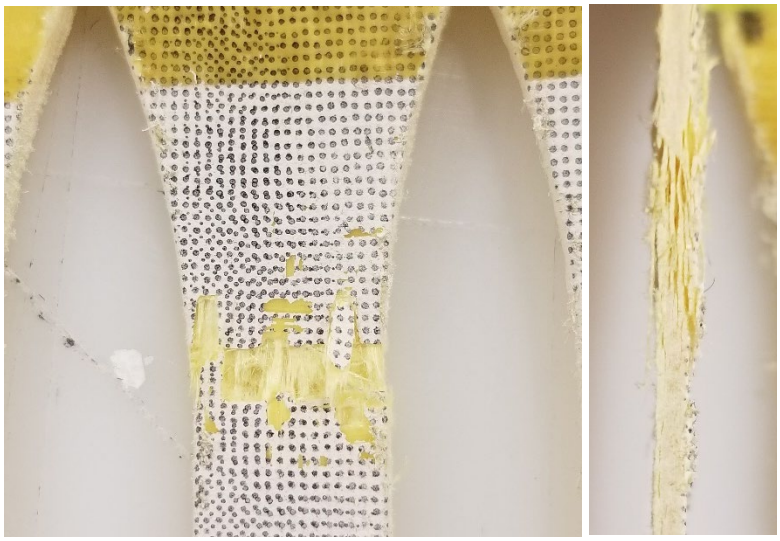

Figure 7: Close up views of failure region in tensile sample

Eighteen samples were tested between the two laminates, and they displayed a linear stress-strain curve to failure. Figure 8 shows that all of the samples failed between 1.4% and 1.8% strain. While these strain

results may be lower than would be expected when compared to the published values for Kevlar® yarns, it is well known in the literature that the strength properties of Kevlar®/epoxy laminates are dependent on the interfacial bonding between the matrix resin and the fiber. For instance, Fouad et. al [9] found strain at failure of 1.17% when testing a Kevlar®/epoxy composite, and attribute the lower than expected tensile results to low wettability of the fiber by epoxy, resulting in a weaker bond than expected. A more in-depth review of the literature related to Kevlar composites that gives additional information on the importance of the interfacial bond can be found in Singh and Samanta should the reader wish further information on the topic [10]. See figure 7, it appears that interlaminar separation could have been occurring during testing, and could also contribute to results that are different from what was expected. Due to budget and time constraints, no additional work was conducted to further understand the failure mechanisms, but would be a consideration for future work.

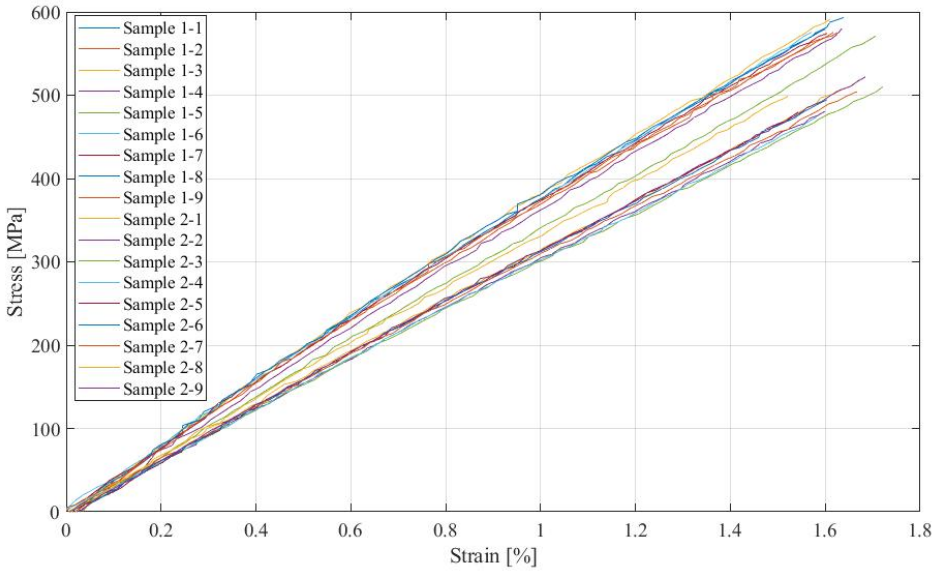

Figure 8: Stress vs strain graph for laminates T-P-1 and T-P-2 tensile samples with layups $[(0/90)]_6$

The linear portion of the stress-strain curves ranging from 0.2% to 0.4% strain was used to calculate the Young's modulus of the Kevlar weave. This strain region is boxed and highlighted in black in Figure 9.

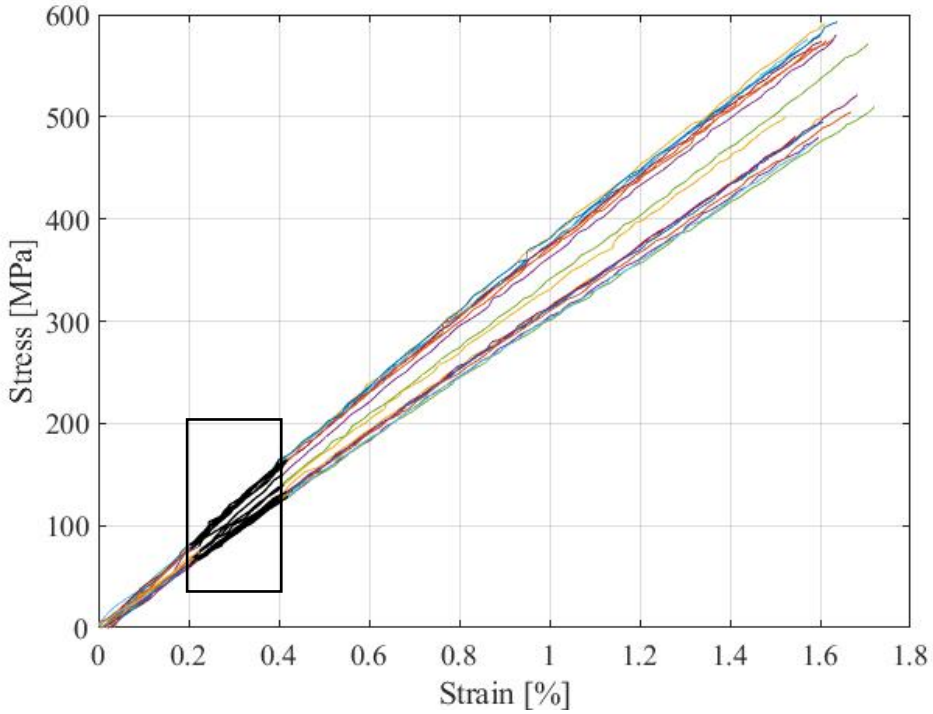

Figure 9: Stress vs strain graph for laminates T-P-1 and T-P-2 tensile samples showing the linear region used for modulus estimation. The box indicates the region used for modulus calculation.

The average Young's modulus for the samples across T-P-1 and T-P-2 was 35.8 GPa with a standard deviation of 3.7 GPa. The average strength was 539 MPa with a standard deviation of 42.6 MPa. Table 3 provides the tensile modulus and strength for each of the samples from T-P-1 and T-P-2.

Table 3: Tensile modulus and strength results from laminates T-P-1 and T-P-2

Tensile Samples		
Sample	**E [GPa]**	**σ_t [MPa]**
1-1	40.3	579.4
1-2	38.5	575.7
1-3	39.6	591.7
1-4	37.2	580.9
1-5	35.6	571.1
1-6	39.2	575.8
1-7	40.6	574.1
1-8	41.3	593.2
1-9	40.5	575.2
2-1	31.3	519.1
2-2	31.6	480.6
2-3	31.0	510.2
2-4	31.4	474.3
2-5	32.9	480.1
2-6	33.1	495.0
2-7	32.2	504.6
2-8	34.1	499.9
2-9	33.3	521.8
Average	**35.8**	**539.0**
Std. Dev	**3.7**	**42.6**

Shear Samples

Eight shear samples were tested from plate S-P-1. The stress-strain curves had a linear region below 2% strain and proceeded to have a shift to nonlinearity beyond that (see Figure 10). The failure strains ranged from 4% to 13%. The shear modulus was calculated from the linear portion of the stress-strain curve.

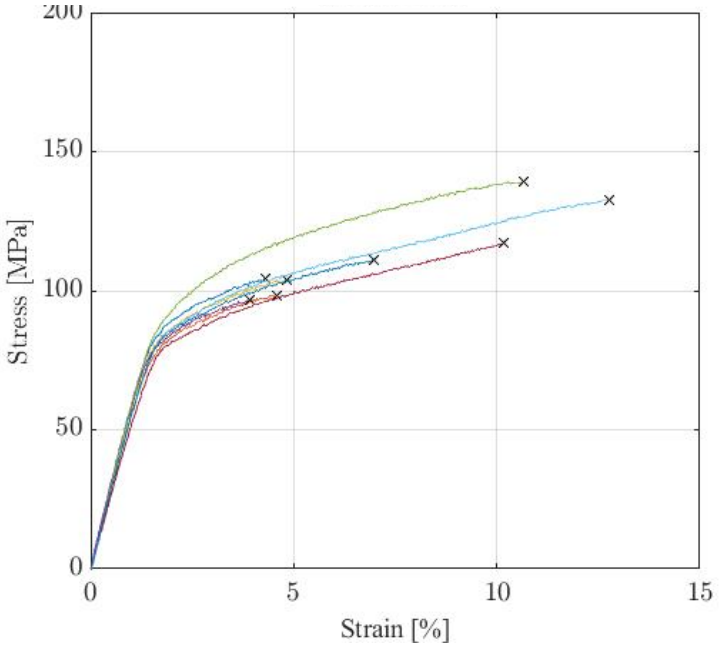

Figure 10: Stress vs strain for samples from laminate S-P-1 with layup $[(\pm 45)]_8$

The average shear modulus from the tested samples was 5.67 GPa with a standard deviation of 0.4 GPa. The shear strength averaged to 112.9 MPa with a standard deviation of 14.7 MPa. Table 4 provides the shear modulus and strength for each tested sample in plate S-P-1.

Table 4: Shear modulus and strength for laminate S-P-1

Shear Samples		
Sample	G_{12} **[GPa]**	τ_{12} **[MPa]**
1	6.29	104.6
2	5.65	98.4
3	5.03	104
4	5.94	96.5
5	6.09	139.4
6	5.38	132.4
7	5.31	116.9
8	5.7	111
Average	**5.67**	**112.9**
Std. Dev	**0.4**	**14.7**

Compression Samples

Eleven compression samples were tested to failure that were produced from plate CF-P-1. While the plate produced 12 samples, 1 sample was used to test the fixture setup. Therefore, the numbering between the data and the labeling on the samples in Sharpie (seen in Figure 11) is off by one. Generally, the ends of the samples that were directly in contact with the crush platens failed by crush and eventual delamination. The delamination was primarily seen along the exterior edge between the first few plies and presents itself

as layers peeling away from the sample (see Figure 12). This is a common occurrence when testing composite samples with this fixture and is typically mitigated by testing tabbed specimens for strength. In this present case, the primary objective was to obtain the compressive modulus, hence no tabbed specimens were tested. The strength data are reported for interest, but should not be taken as representative of the material strength of the Kevlar-epoxy material.

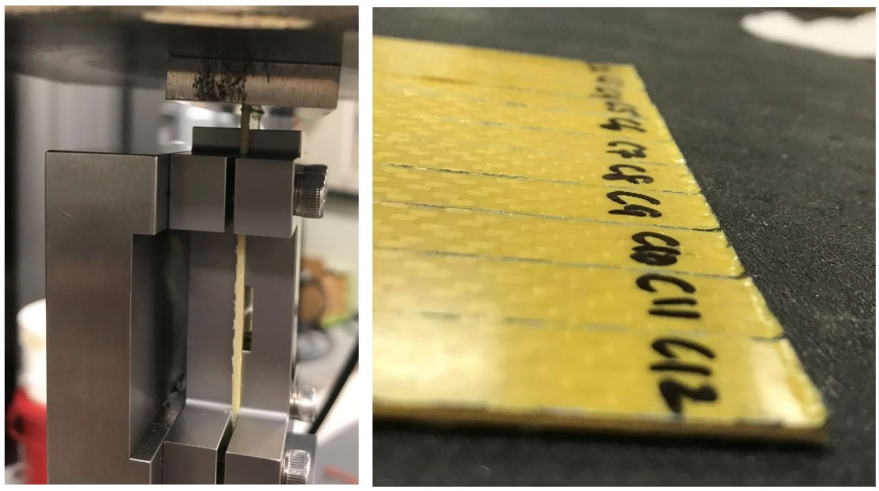

Figure 11: Crushing of contact ends in compression samples from laminate CF-P-1

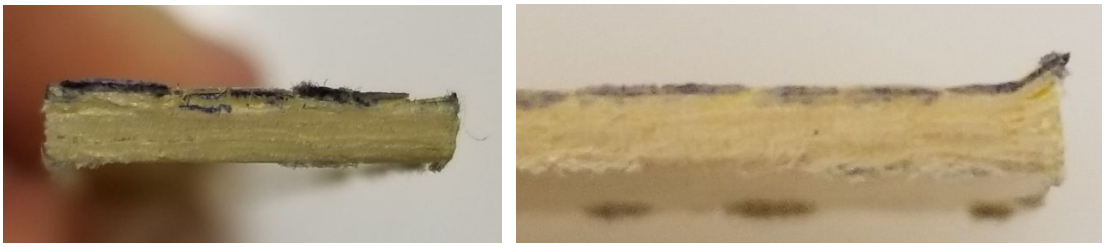

Figure 12: Front and side view of failed compression sample

The stress-strain curves for the compression samples showed a small strain region of little load. This is attributed to zero-load displacement when the fixture is settling before applying load to the sample. The stress-strain curves (see Figure 13) show nonlinearity past 0.5% strain, but failure occurs between 0.75% to 1.4% strain.

It is immediately evident that sample C3 has an uncharacteristically low stress-strain curve. This sample buckled instead of being crushed because the test fixture screws were not tightened sufficiently to constrain out-of-plane motion. Figure 14 shows the buckled sample (labeled sample C4 in the picture). The buckling failure for sample C3 (labeled C4) in the picture resulted in that sample being omitted from the modulus and strength calculations.

Sample C1 has a stress-strain curve that also presents a bit differently from the group of samples. However, there was no sign of the sample failing in a different manner like sample C3. Therefore, that sample was included in the modulus and strength calculations.

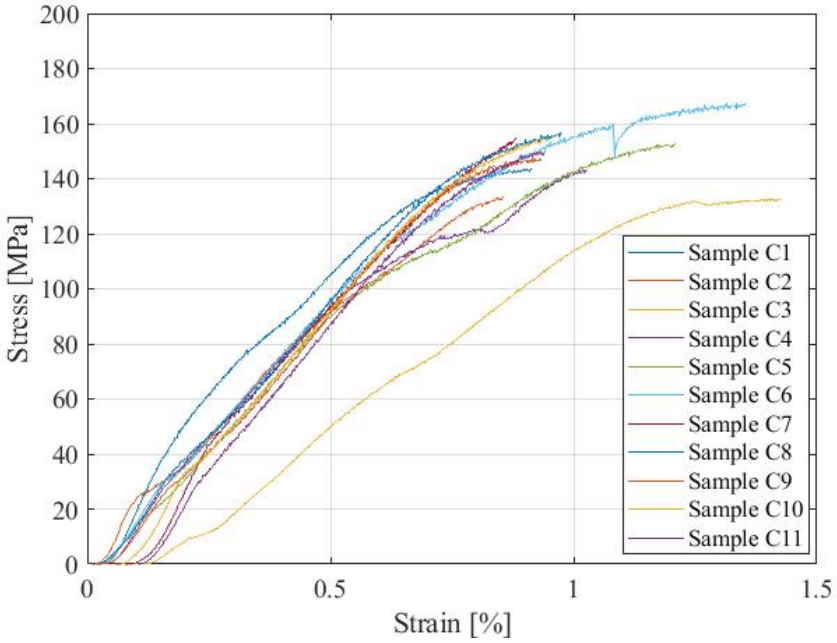

Figure 13: Stress vs strain graph for compression samples from laminate CF-P-1 with layup $[(0/90)]_6$

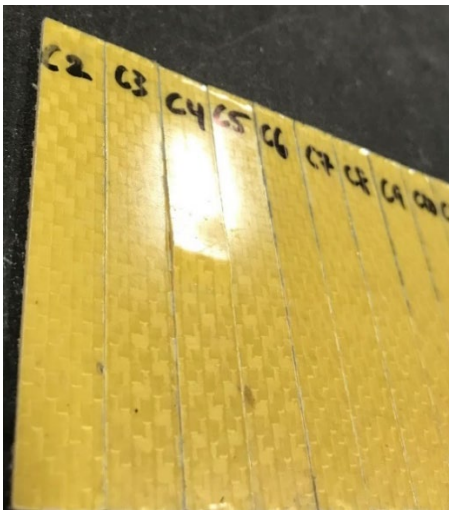

Figure 14: Sample C3 (labeled C4 in Sharpie) buckled during testing resulting in a lower stress-strain curve

The slope of the stress-strain curve for the compression samples was taken between 0.3% to 0.5% strain because of the nonlinearities seen below 0.2% strain. The data used to estimate the compressive modulus of the samples is highlighted in black in Figure 15.

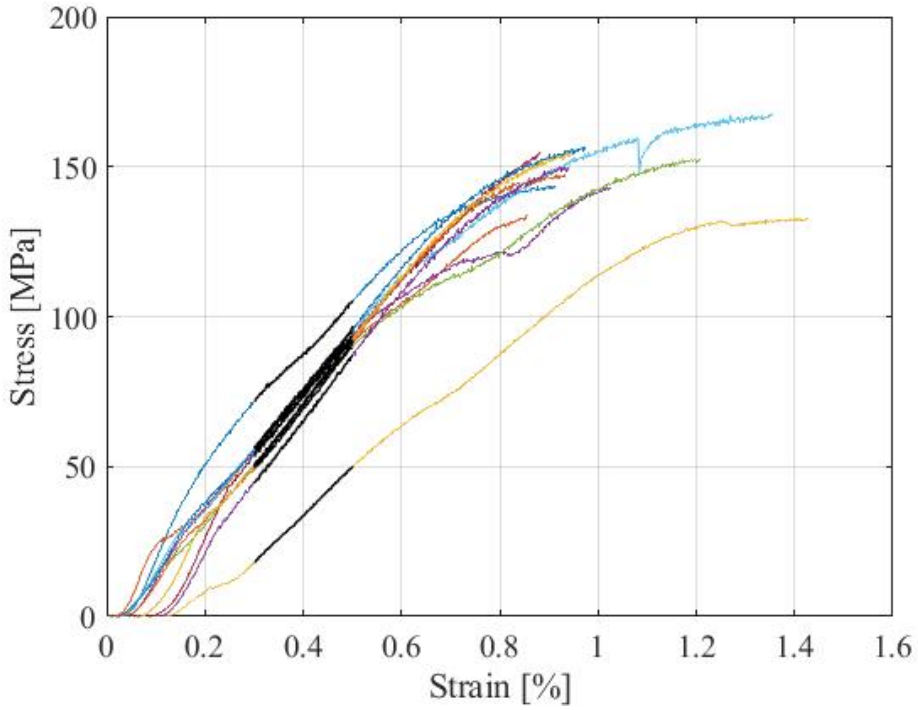

Figure 15: Stress vs strain graph for compression samples from laminate CF-P-1 showing linear region used for modulus estimation

The average compressive modulus was 19.7 GPa with a standard deviation of 1.6 GPa, while the average compressive strength was 150.6 MPa with a standard deviation of 8.8 MPa. Table 5 presents the stiffness and strength data for each of the compression samples from plate CF-P-1.

Table 5: Compressive stress and modulus results for samples from laminate CF-P-1

Compression Samples		
Sample	**E [GPa]**	**Strength [MPa]**
C1	16.1	143.8
C2	18.0	133.9
C3	-	-
C4	19.0	143.2
C5	20.1	152.8
C6	19.8	168.0
C7	19.9	155.0
C8	20.8	156.8
C9	21.0	147.6
C10	21.4	154.7
C11	21.3	150.1
Average	**19.7**	**150.6**
Std. Dev	**1.6**	**8.8**

Flexure Samples

Ten flexure samples were created from plate CF-P-1. The first 5 samples were tested at a support span of 76.8 mm as is recommended by ASTM D7264. Per the discussion in Carlsson et al, [8] this value is a suitable starting point for measurement of high strength composites. The span to thickness ratio, L/t, was roughly 50. However, the samples were so flexible, they did not fail at this support width. Instead, the samples slipped between the supports before failure occurred. Because of this, strength values were not recorded for the samples tested at the support span of 76.8 mm. The remaining five flexure samples were tested at a support span of 32.2 mm to capture failure. The new the span-to-thickness ratio was 20, and Euler-Bernoulli beam theory could still be applied. In Figure 16, there is an obvious difference between the stress-strain curves associated with each span. The curves tested at the reduced span reach a higher strain and stress. The linear regions of both sets of data show similar slopes though.

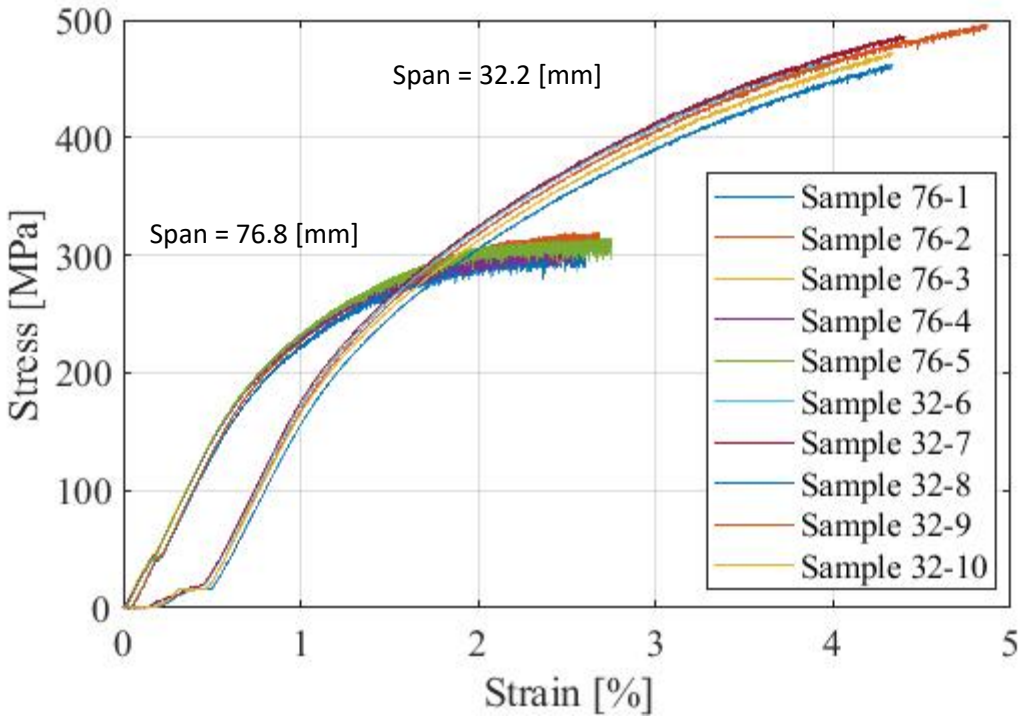

Figure 16: Stress vs strain graph for flexure samples at 76.8 mm support span and 32.2 mm support span cut from laminate CF-P-1 with layup $[(0/90)]_6$

The linear region of the stress strain curves between 0.5% and 0.7% were used to estimate the flexural stiffness. Figure 17 shows the linear region highlighted in black.

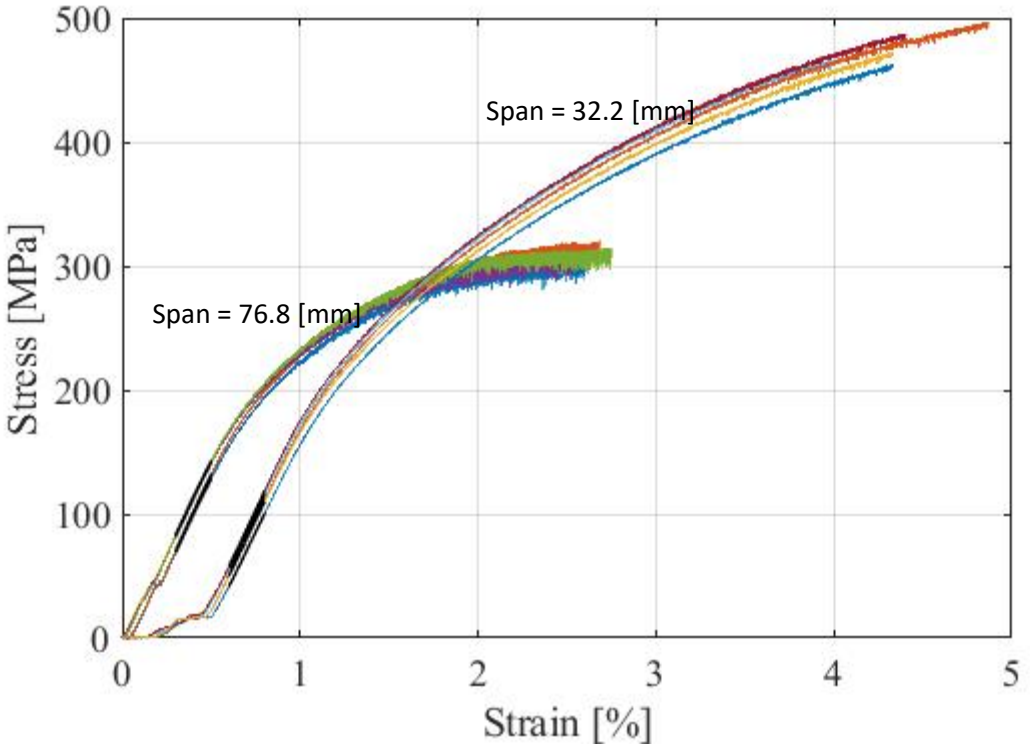

Figure 17: Stress vs strain graph for flexure samples from laminate CF-P-1 showing linear region used for modulus estimation

The average flexural modulus for samples tested at a support span of 76.8 mm was 30.4 GPa with a standard deviation of 0.4 cxGPa. Similarly, the average flexural modulus for samples tested at the reduced support span was 30.0 GPa with a standard deviation of 0.3. These values are close enough to assume the support span did not affect the flexural modulus. The samples with a reduced span had a strength of 477.3 MPa with a standard deviation of 12.9 MPa. Table 6 shows the flexural modulus and strength for each of the samples coming from plate CF-P-1.

Table 6: Flexural stress and modulus results for samples cut from laminate CF-P-1

	Flexure Samples		
	Sample	**E_f [GPa]**	**Strength [MPa]**
Span 76.8 [mm]	76-1	30.2	
	76-2	31.0	
	76-3	30.1	
	76-4	30.2	
	76-5	30.7	
	Average	**30.4**	
	Std. Dev.	**0.4**	
Span 32.2 [mm]	32-6	30.0	466.2
	32-7	30.4	486.7
	32-8	29.4	462.9
	32-9	30.3	497.2
	32-10	29.9	473.5
	Average	**30.0**	**477.3**
	Std. Dev.	**0.3**	**12.9**

Manufacturing Method Tensile Property Comparison

Several laminates were manufactured in the oven or autoclave to compare to the properties produced from the laminates that were manufactured in the press. The test methodology was the same as previously described, and the DIC was used to record strain measurements on the samples. The stress versus strain plots were produced for each set of samples and can be seen in Figure 18 through Figure 21.

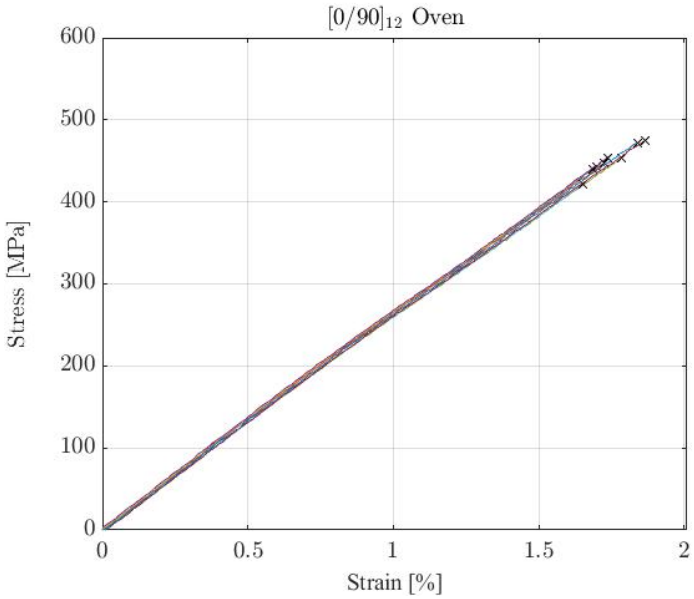

Figure 18: Stress vs strain plot for samples from laminate T-O12-1

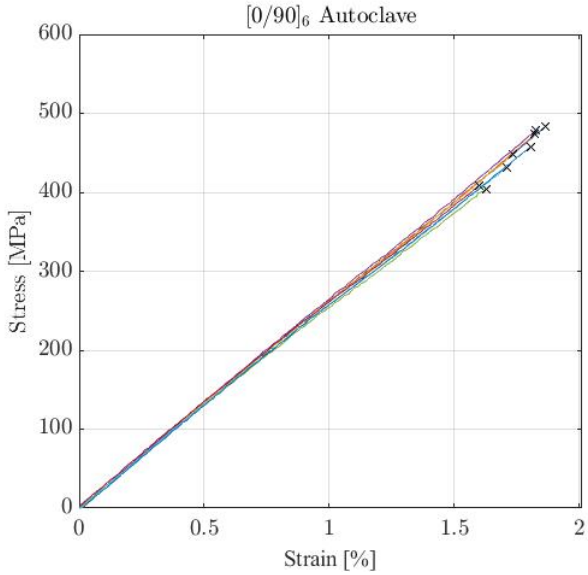

Figure 19: Stress vs strain graph for samples from laminate T-A-1

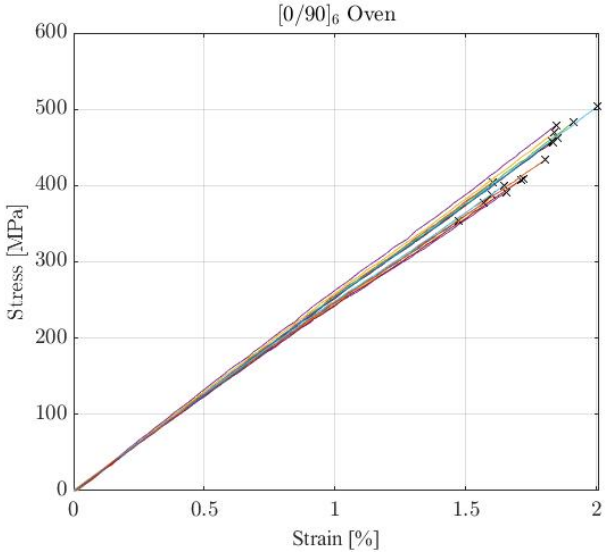

Figure 20: Stress vs strain results for samples from laminates T-O6-1 and T-06-2

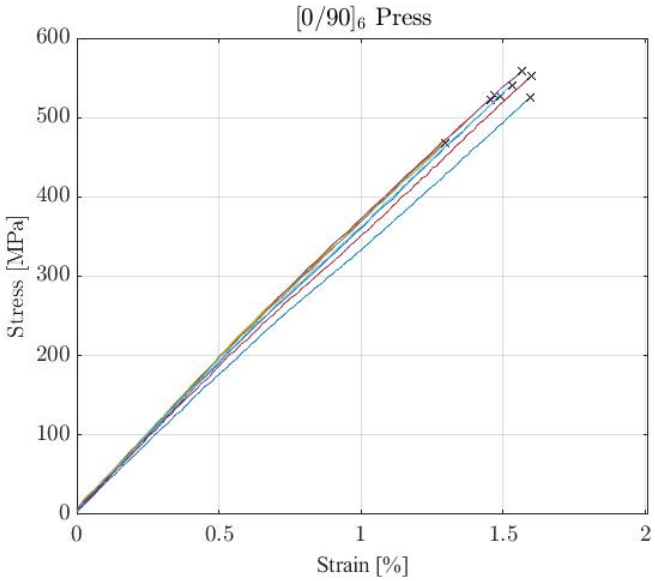

Figure 21: Stress vs strain results for samples from laminate T-P-3

Comparing the Young's modulus between the manufacturing methods (see Figure 22) reveals that the samples made in the press yielded a higher Young's modulus than the other manufacturing methods. In addition, the pressed samples also have the highest strength (see Figure 23). These results can be seen numerically in Table 7. The first row that is bolded shows the data of T-P-1 and T-P-2 from the standard characterization with the dog bone samples. These results are consistent with the other pressed samples from T-P-3 that used rectangular dimensions with fiberglass tabs.

The resin was designed to be a snap-cure system used in compression molding for automotive parts. As the resin was optimized for a specific manufacturing process, it makes sense that the material properties would be best (highest stiffness and strength) in samples made with that process. In addition, the oven and autoclave did not reach the pressures achieved during compression molding.

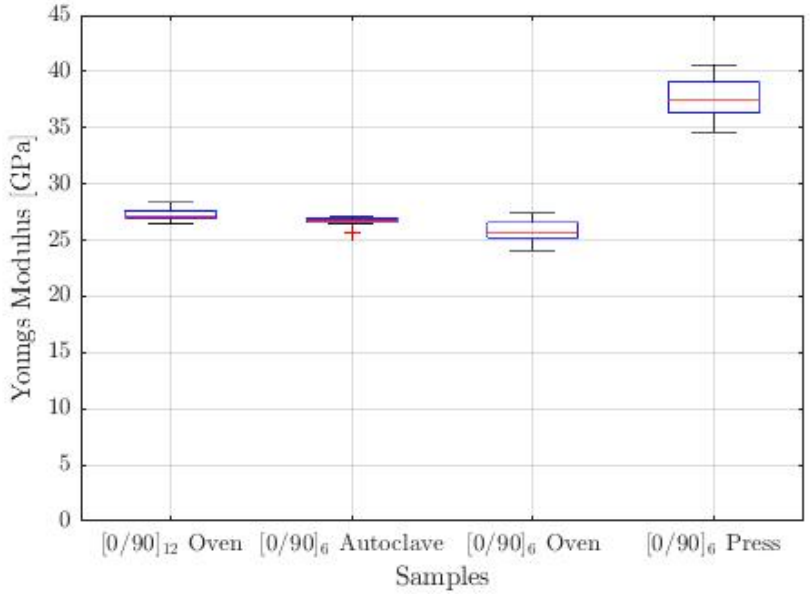

Figure 22: Comparison of stiffness for different manufacturing methods

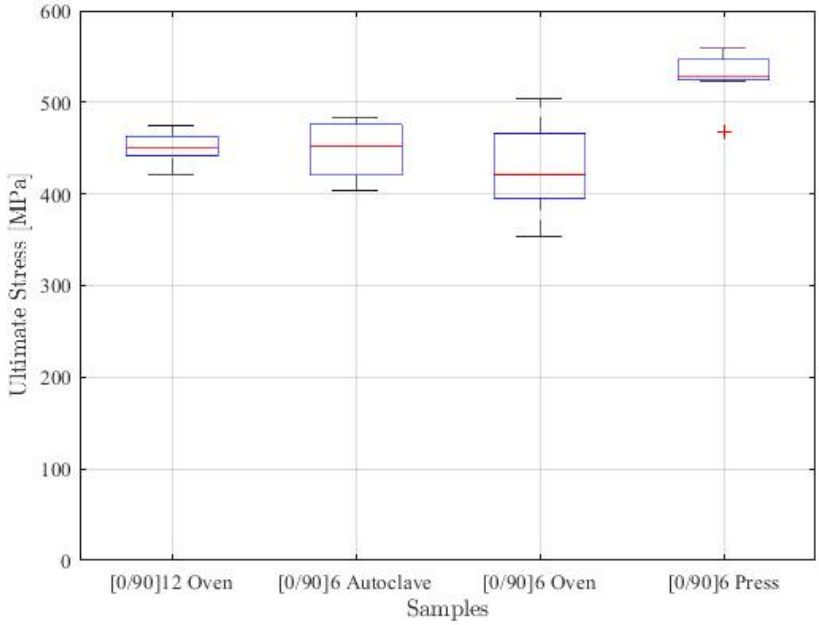

Figure 23: Comparison of strength for different manufacturing methods

Table 7: Summary of tensile properties

Plate(s)	E [GPa]	Std Dev. [GPa]	Strength [MPa]	Std Dev. [MPa]
T-P-1 **T-P-2**	**35.8**	**3.7**	**539.0**	**42.6**
T-O12-1	27.16	0.57	450.01	17.21
T-A-1	26.78	0.44	452.5	30.67
T-O6-1 T-O6-2	25.73	0.93	421.02	43.99
T-P-3	37.41	2.07	527.69	27.72

Conclusion

This report section provides details regarding the material characterization of a Kevlar weave with a thermoset resin system commercially available from Hexion. Experimental material characterization of the tensile, shear, flexure, and compression behavior was completed with samples made from the Kevlar weave with Hexion EPIKOTE resin. Combining the results from the previous sections yields Table 8, which contains the calculated stiffnesses, strengths and standard deviations for each test completed. These values are requirements in material models for a majority of finite element simulation software systems. See the Commercialization section at the end of the report for discussion on recommended next steps.

Table 8: Summary of material properties from characterization tests

Sample Type	Modulus [GPa]	Std. Dev [GPa]	Strength [MPa]	Std. Dev. [MPa]
Tension	35.8	3.7	539.0	42.6
Shear	5.67	0.42	112.9	15.7
Flexure, 76.8mm span	30.3	0.4		
Flexure, 32.2mm span	30.0	0.3	477.3	12.9
Compression	19.7	1.6	150.6	8.8

Appendix

Average sample dimensions for dog-bone tensile, flexure and compression samples are included below.

Table 9: Dimensions of tensile samples from laminates T-P-1 and T-P-2

	Thickness (mm)		Width (mm)	
Sample Number	T-P-1	T-P-2	T-P-1	T-P-2
1	1.39	1.72	10.1	10.17
2	1.41	1.77	10.1	10.14
3	1.4	1.81	10.1	10.14
4	1.47	1.76	10.13	10.16
5	1.53	1.63	10.06	10.1
6	1.48	1.71	10.12	10.15
7	1.42	1.72	10.11	10.16
8	1.4	1.72	10.11	10.14
9	1.38	1.71	10.11	10.14
Average	**1.43**	**1.73**	**10.1**	**10.15**

Table 10: Dimensions of flexure samples from laminate CF-P-1

	Sample	Thickness [mm]	Width [mm]	Length [mm]
76.8 mm Support Span	1	1.54	12.96	100.6
	2	1.54	13.11	100.7
	3	1.54	13.1	100.45
	4	1.55	13.14	100.6
	5	1.57	13.08	100.35
	Average	**1.54**	**13.1**	**100.49**
32.2 mm Support Span	6	1.58	13.16	100.51
	7	1.62	13.13	100.46
	8	1.61	13.11	100.51
	9	1.63	13.09	100.85
	10	1.65	13.1	100.7
	Average	**1.62**	**13.11**	**100.56**

Table 11: Dimensions of compression samples from laminate CF-P-1

Sample	Thickness [mm]	Width [mm]
1	1.49	12.93
2	1.49	12.83
3	1.5	12.84
4	1.49	12.87
5	1.5	12.88
6	1.51	12.86
7	1.52	12.89
8	1.54	12.82
9	1.54	12.88
10	1.58	12.86
11	1.59	12.86
Average	**1.52**	**12.87**

Additional rheological study of the epoxy resin system used in this phase of the work had been planned as part of the original research proposal. However, availability of research quantities of resin was limited during the project time-frame, so this work was not conducted. The resin vendor has rheological data available to aid in usage of their material.

Subtask 7.3.4 Kevlar®/Thermoplastic Prepreg Characterization

Executive Summary

The IACMI 7.3.4 project between DuPont and Purdue University had Purdue's Manufacturing Design Laboratory (MDLab) manufacture 600 meters of Kevlar®/VZL-36D (polyamide based) unidirectional prepreg tape and characterize the resulting prepreg's mechanical, thermoelastic, and rheological properties. The directional: tensile, compressive, flexure, and coefficient of thermal expansion properties were determined along with the shearing properties of the prepreg and rheological properties of the neat resin. These properties can be considered for inclusion in a "material card" to inform finite element modeling and simulation software. A summary of the mechanical material properties is included in Table 12. We note that while the mechanical properties are considerably lower than for the woven prepreg, this is likely caused by lower fiber volume fraction in the UD prepreg relative to the woven prepreg. The UD prepreg fiber volume fraction was measured to be 35%. While the fiber volume fraction of the woven prepreg was not measured, an estimate of 45% is reasonable and would account for the differences in elastic constants observed between the UD and woven prepregs. This report provides details regarding the test procedures and analysis used to determine these mechanical and thermoelastic properties.

Table 12: Mechanical testing summary for VZL-36D/Kevlar® prepreg (V_f = 0.35)

Sample Type	Modulus (GPa)	Strength (MPa)	ν_{12}
Tension [0°]	27.41 ± 0.80	463.8 ± 28.4	0.45 ± 0.05
Tension [90°]	3.55 ± 0.52	30.8 ± 2.2	
Compression [0°]	10.47 ± 1.39	131.5 ± 6.5	
Compression [90°]	3.13 ± 0.30	89.7 ± 8.0	
Flexure [0°]	21.3 ± 0.7	345.5 ± 39.2	
Flexure [90°]	3.58 ± 0.42	45.8 ± 4.0	
Shear	1.12 ± 0.06	50.1 ± 4.8	

Introduction

Kevlar®/polyamide thermoplastic unidirectional prepreg tape was manufactured at the Manufacturing Design Laboratory (MDLab) at Purdue University as part of the IACMI 7.3.4 project. The manufacturing conditions were reported for repeatable processing of this material system in the future. The resin was a polyamide-6, VZL-36D, which was specially formulated for to aid in processing. The laminates made from the prepreg tape were characterized for its mechanical properties (tensile, flexural, shear, and compressive – stiffnesses and strengths). The experimentally measured mechanical, thermoelastic and rheological properties are reported along with the manufacturing process conditions, sample preparation, analysis method, and discussion regarding the experimental results.

Background

The goal of the IACMI 7.3.4 project was to establish manufacturing conditions for Kevlar®/VZL-36D prepreg and characterize its material properties for potential future use within performance simulations.

Prepreg Manufacturing

The thermoset and thermoplastic prepreg tape line at the Manufacturing Design Laboratory (MDLab) spans 10m and was designed to study manufacturing conditions for unique resin and fiber combinations. The line typically operates at speed of 0.5 – 2.5m/min (1.5 – 8FPM) and produces up to 75mm wide tape, with a thickness up to 1mm. The prepreg tape line was designed to process carbon, aramid, and glass fibers with any thermoplastic or thermoset resin, including high performance thermoplastics, such as PEEK. The impregnation die can be refitted to produce composite strands with a diameter up to 3mm for discontinuous fiber composites (long discontinuous unidirectional fiber thermoplastics, LFT). Additionally, the resin extrusion system was designed to operate with a second melt pump to process two-part resin systems.

The fiber creel was loaded with 26 bobbins of commercially available Kevlar® 49 fiber (DTEX 3160-1333-0-49, DEN 2840). These fibers were provided by DuPont and each yarn was pre-tensioned to 500g. An image of the fibers loaded on the creel is shown in Figure 24. The fibers are collimated using two combs on the spreader unit before entering the fixed bar spreaders to evenly distribute the individual yarns into a uniform web, as shown in Figure 24. Since Kevlar® fibers can hold up to 5wt% water, they need be dried before processing, in addition the spreader was equipped with an IR lamp which allowed the fibers to reach a temperature of 175°C to dry the Kevlar® fibers before entering the impregnation die. The fiber temperature was measured at the surface using a handheld infrared thermometer. The dried fibers were necessary to eliminate negative influence on the properties.

Figure 24: Overview image of the prepreg tape line's 48 position creel (left) and fixed bar fiber spreading unit (right).

The resin used for this project was VZL-36D (polyamide-6) resin which was provided by DuPont. The polyamide-6 resin was pre-dried at 80°C for 14 hours at ambient pressure with no purge gases used before being extruded. A ¾" single screw (non-vented, non-mixing) extruder (36 L/D) heated the resin to a temperature of 270°C and pressurized the polymer to 800psi for the melt pump. The extruder has 4 heating zones, with the following temperature profile used: Zone 1 – 250°C, Zone 2 – 260°C, Zone 3 – 265°C, and Zone 4 – 270°C. The melt pump (0.6cc/rev) was used as a metering device to control the flow of molten polymer into the impregnation die. The melt pump calibration curve is provided in Appendix A1.

An overview of the extruder, melt pump, and impregnation die assembly can be seen in Figure 25. The resin was pumped into the fiber bed by controlling the tension in the fibers and dragging the fibers across the ridges in the die, effectively pumping the resin into the fiber bed. The lips of the die were adjustable with three set screws to allow for production of prepreg up to 1mm thick. An example of the Kevlar®/VZL-36D prepreg exiting the die is shown in Figure 26. Then the tape went through a series of rollers to ensure the tape exited the die level. Tape that exited the die at an angle resulted in excess resin on one surface while the other surface was deficient of resin, which resulted in warped and unsatisfactory tape.

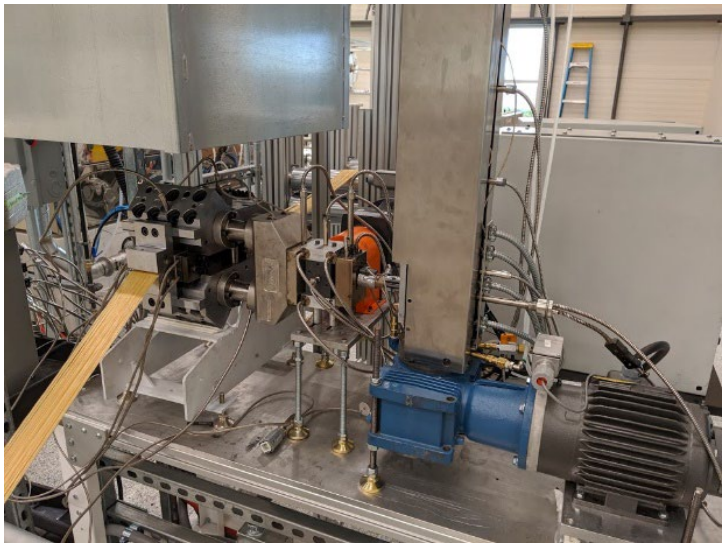

Figure 25: Overview image of the prepreg tape line's extruder, melt pump, and impregnation die.

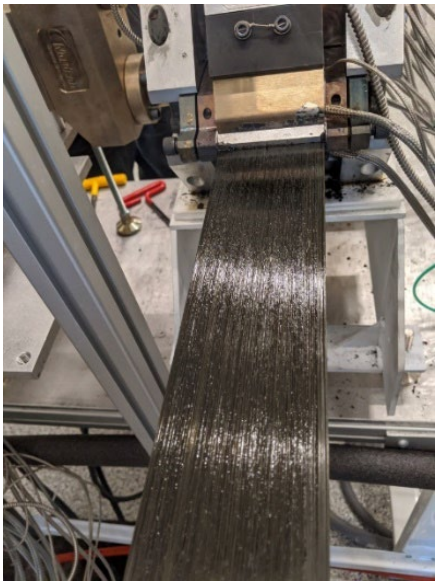

Figure 26: Kevlar®/VZL-36D prepreg exiting the impregnation die.

The addition of the rollers after the die had to be adjusted to avoid inconsistent fiber volume fractions along the width of the prepreg tape. Figure 27 labels the different regions of the prepreg tape, displayed a representative micrograph of the prepreg tape, and the resulting fiber volume fractions for the different prepreg sections along its width. The microscopy images were analyzed in ImageJ and used image thresholding to determine the fiber volume fraction. ImageJ thresholding requires a non-color (8-bit) image and the threshold values to be specified by the user. Threshold values can range from 0 – 255 (for 8-bit) and can differ depending on the type of sample and microscope settings. Typical threshold values used for the Kevlar®/VZL-36D prepreg ranged from 150 – 160.

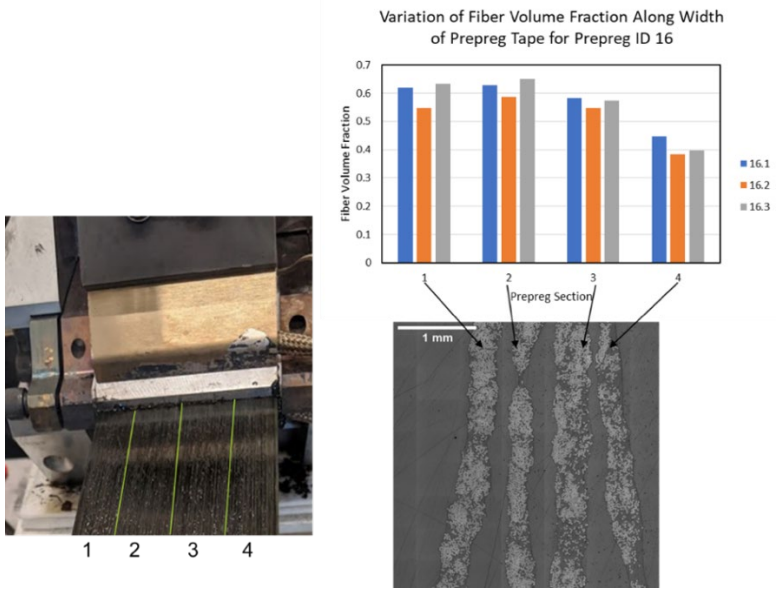

Figure 27: Example from prepreg ID 16 showing the fiber volume fraction varying at different locations along the prepreg width. The spacing between prepreg strips is a result of the mounting epoxy, not because there is a resin rich layer at the prepreg surface.

The prepreg line operated across a range of operating speeds to determine optimal manufacturing conditions for the Kevlar®/VZL-36D prepreg. The melt pump was operated from 10 – 60 RPM while the line speed was 1.5 – 8 FPM. The impregnation die length is 1ft which corresponded to a fiber residence time inside the die from 8 to 40 seconds. While the line and pump speeds were varied over various manufactured prepregs, the impregnation die was consistently heated to 310°C. This temperature was chosen based on the recommendation of Karl Chang at DuPont. An abbreviated summary of the prepreg line operating conditions is shown in Table 13, while a complete list is shown in Appendix A1. The expected fiber volume fraction in Table 13 was based on the pump to puller ratio and number of yarns being used (26 yarns). The expected prepreg fiber volume fraction was checked at two pump-to-puller ratios and found agreement with this estimate. The comparison of estimated to measured fiber volume fraction is shown in Figure 28.

Table 13: Kevlar®/ VZL-36D prepreg manufacturing conditions

Prepreg ID	Pump Speed [RPM]	Line Speed [FPM]	Yarn Count	Die Temp [°C]	Expected V_f
18	14.5	2.0	26	310	0.51
19	14.5	2.0	26	310	0.51
20	13.5	2.0	26	310	0.52
21	14.5	2.0	26	290	0.51
22	19.0	2.0	26	310	0.43
23	30.0	2.0	26	310	0.33
24	30.0	2.0	26	310	0.33
25	30.0	2.0	26	310	0.33
26	60.0	4.0	26	310	0.33
27	42.0	3.0	26	310	0.34
28	40.0	3.0	26	310	0.35
29	15.0	1.5	26	310	0.42
30	45.0	4.5	26	310	0.42
31	12.0	2.0	26	310	0.55

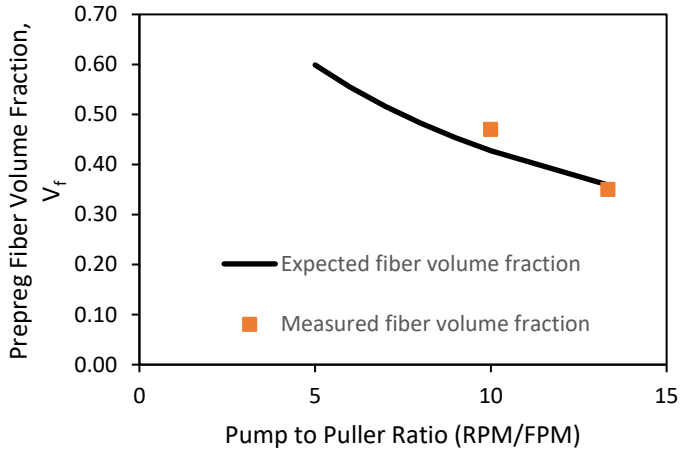

Figure 28: Estimated fiber volume fraction compared to measured fiber volume fraction for different pump to puller ratios. Assuming 26 yarns of Kevlar® were used.

Specimen Preparation

The manufactured Kevlar®/VZL-36D prepreg was consolidated into flat, 10" square laminates for coupon preparation. The prepreg was dried before compression molding by holding the tape at 80°C for 14 hours. A total of 31 laminates were produced from 15 different iterations of prepreg to identify ideal prepreg manufacturing and compression molding conditions. The prepreg that produced the best unidirectional laminates without cracking were laminates made from prepreg ID 28.2. This prepreg had a consistent fiber volume fraction of 0.35 along the width of the tape. While this was low, other attempts with prepreg at a higher fiber volume fractions resulted in cracked laminates. The ideal compression molding conditions were to preheat the upper press platen to 275°C and the lower to 270°C. Furthermore, it was necessary to perform a hand layup on a preheated mold at 280°C, to ensure consistent consolidation. It was noted that attempting to use a cold tool would result in poor consolidation or prolonged exposure to high temperatures and degrade the material. Pressure was removed once the mold cooled to 210°C and the plate was demolded once the mold was below 45°C. Once the mold reached 240°C (the mold would cool down considerably during the hand layup), 60psi was applied for 10 minutes. The final mold

temperature before cooling was typically 250°C. A summary of compression molding conditions can be found in Table 14, compression molding conditions for untested laminates can be found in Appendix A1.

Table 14: Pressing conditions for Kevlar®/VZL-36D prepreg

Plate #	Prepreg ID	Layup	Press Force [ton]	Peak Press Temperature [°C]
23	28.2	$[0]_6$	3	246
24	28.2	$[0]_6$	3	250
25	28.2	$[0]_6$	3	250
26	28.2	$[0]_6$	3	248
31	28.2	$[0,90]_{2S}$	3	248

Five plate samples were compression molded using a 30-ton press for mechanical and thermoelastic characterization. Four laminates (Plate # 23 – 26) had a unidirectional layup and were composed of 6 plies to determine the 0° and 90° properties. Approximately 3.5 strips of prepreg were used per ply, since the tapes were ~2.8" wide. The half strip location in the ply was alternated to stagger the prepreg and avoid any defects in the prepreg being concentrated in one area through the thickness of the laminate plate. The fifth sample (Plate #31) was a symmetric, cross-ply laminate composed of 8 plies to determine the $\pm$ 45° shear properties. The layups used in this characterization are shown in Table 14.

Normally, test coupons would be cut using the surface grinder, however the IACMI 7.3.3 project noted the Kevlar® material tended to fray with that method. Instead, the waterjet was used to cut test coupons from each plate, which made clean cuts. The cut profiles used, and sample naming convention are shown in Figure 29. Typically, tabbed samples are used for tensile testing, however, the 0° and 90° tensile coupons were cut into dog-bones with dimensions following ASTM D638-14 for Type I. Dog-bone samples were used to determine accurate tensile stiffness values of the composite samples. We are well aware that the dog-done samples are not optimal for strength characterization and should not at this stage be considered to be fully representative, even though no shearing or unexpected deformation was observed in the clamping area. Any samples with failure near to the clamping area was disregarded. The compression samples were prepared following the Modified ASTM D 695 Compression Test, which calls for samples approximately 100mm long and 12.5mm wide. The flexure samples were prepared following ASTM D7264 with dimensions approximately 200mm long and 12.5mm wide. Shear samples were approximately 150mm long (50mm shorter than recommended by ASTM D3518-18) and 25.4 mm wide. The shortened samples were necessary because of limited plate size and requirement to cut the samples at a 45° angle from the 10" plate. An example of the cut plate and naming convention are shown in Figure 30. Thickness and width measurements for all mechanical testing samples were measured in three locations along the gage length and were averaged and reported in the Appendix A2. The coefficient of thermal expansion (CTE) samples were cut to 37.5mm squares. All samples were dried at 80°C prior to testing for 14 hours.

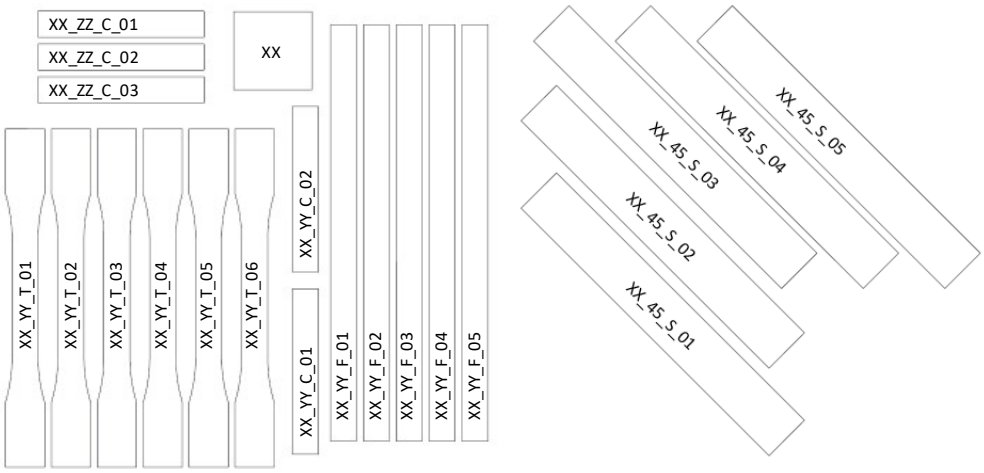

Figure 29: Waterjet cutting profile for unidirectional samples (left) and ± 45° samples (right). File naming convention: XX = laminate number, YY = fiber orientation (0° or 90°), ZZ = fiber orientation (90° or 0°), T = tensile test, C = compression test, F = 3pt bending test, and S = shear test.

Mechanical testing sample gauge sections were spray painted white and speckled with black ink, while the CTE samples were speckled with a fine layer of white, temperature resistant paint. The speckle on the sample surface was used to determine the surface strains during testing. The CTE samples were speckled using the spray paint, because full coats of spray paint result in tests measuring the CTE of the paint, rather than the sample.

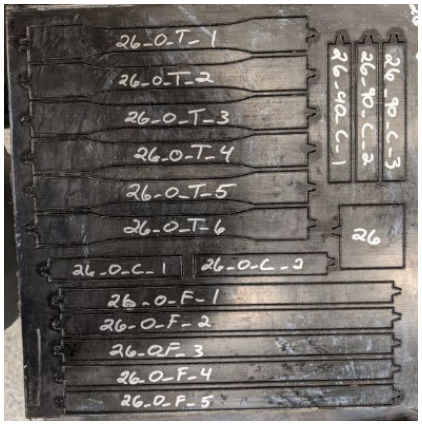

Figure 30: Plate 26 after being water-jetted, showing the naming convention used for unidirectional samples.

The unidirectional laminate laminates 23 – 26 had their fiber volume fraction checked in five different regions. The resulting fiber measurements are shown in Table 15. The fiber volume fraction between each plate ranged from 0.325 – 0.352, which was an acceptable variation in the fiber content. Additionally, fiber volume fraction throughout the individual laminates was observed to not vary significantly. The fiber volume fraction for the resulting laminates was low, but laminates with higher fiber volume fractions would crack. For this reason, the prepreg with a fiber volume fraction of 0.35 was characterized.

Table 15: Fiber volume fraction from manufactured laminates from prepreg ID 28 showing consistent fiber content throughout the plate and across laminates.

Plate ID	V_f	Plate ID	V_f	Plate ID	V_f	Plate ID	V_f
23.1	0.324	24.1	0.322	25.1	0.353	26.1	0.346
23.2	0.328	24.2	0.372	25.2	0.347	26.2	0.355
23.3	0.315	24.3	0.349	25.3	0.343	26.3	0.342
23.4	0.316	24.4	0.374	25.4	0.39	26.4	0.346
23.5	0.342	24.5	0.345	25.5	0.347	26.5	0.344
Average	0.325	Average	0.352	Average	0.356	Average	0.347

Test Methodology

Digital Image Correlation (DIC) Strain Measurement

Digital image correlation (DIC) was used to measure the surface strains of the sample rather than strain gauges. The samples were sprayed with a light coat of white spray paint. The spray paint can nozzle was kept approximately 8 inches away from the sample surfaces. Multiple light coats of paint were applied to the sample surface using a sweeping pattern to make sure no streaks of paint occurred on the sample surface as described in the "VIC Speckle User Manual" from Correlated Solutions [1]. Coats were approximately every 10 minutes. The paint on the samples was allowed to dry for 1 hour before an ink speckle pattern was applied in a single stroke from the ink stamp roller.

Two 5MP camera were setup to acquire images of the sample during loading. The cameras were adjusted to make sure the gage section of the sample was in the field of view for both cameras. 30 – 40 calibration images were taken using the calibration pattern (patterns from Correlated Solutions) for the VIC 3D calibration, as described in "VIC-3D Easy Guide Setup Procedures for the VIC-3D 5MP Quasi Static System" [2]. The acquired images were post processed in VIC Snap 3D. A region of interest was selected in the gage section of the sample (approximately 25mm long and several millimeters away from the sample edges). The longitudinal, lateral, and shear strains in this region were averaged and reported as discrete values for each image. A copy of the standard operating procedure for DIC prep and analysis at the Composites Manufacturing and Simulation Center is included in Appendix A3.

Tensile Testing

The tensile testing was performed with a 22kip MTS load-frame on samples with a $[0]_6$ or $[90]_6$ layup to determine the directional dependent tensile stiffness and strength properties. A dog-bone coupon geometry was used in order to acquire accurate stiffness measurements. The crosshead displacement rate was set to 2mm/min, as described by ASTM D3039 with the load and displacement data being recorded at 10Hz [3]. Tensile strain (ϵ_t) measurements were recorded using digital image correlation (DIC), where two cameras recorded images in sync with the load vs displacement data. The tensile stress (σ_t) of the sample was calculated from the tensile load (P) and cross section of the sample (width, w and thickness, t). The DIC method was able to calculate the surface strain field from sequential images of the sample. Samples were loaded into the hydraulic grips and secured with Emory cloth to ensure no slipping occurred in the grips. Samples were stressed until the sample could no longer carry significant load. The sample dimensions and load measurements were used to determine the sample stress. Sample stresses vs strain were plotted to determine the Young's modulus (E_t) and ultimate tensile strength in the fiber direction (0° or 1-direction) and transverse (90° or 2-direction). The Young's modulus was defined as the slope of the stress-strain curve in the linear region of the curve.

$$\sigma_t = \frac{P}{wt} \tag{12}$$

$$E_t = \frac{\Delta\sigma_t}{\Delta\varepsilon_t} \tag{13}$$

Shear Testing

The shear testing was performed with a 22kip MTS load-frame with a crosshead displacement of 2mm/min, as described by ASTM D3518 [4]. This test uses samples with a $[\pm 45]_{2S}$ layup and loads them in tension to determine the shear modulus (G_{12}) and strength. Load vs displacement data was recorded at 10Hz and was synced with the captured images with the DIC system. The DIC system was used in the same way as the tensile testing, to determine the surface strains. Samples were loaded in the same manner as the tensile samples.

$$\tau_{12} = \frac{P}{2(wt)} \tag{14}$$

The shear modulus of elasticity was defined as the slope of the shear stress (τ_{12}) – shear strain (γ_{12}) curve in the linear region. The shear strain was defined by the longitudinal strain (ϵ_x) and lateral strain (ϵ_y). The shear strength was measured and reported as the maximum of the stress the sample was able to withstand.

$$\gamma_{12} = \epsilon_x - \epsilon_y \tag{15}$$

$$G_{12} = \frac{\Delta\tau_{12}}{\Delta\gamma_{12}} \tag{16}$$

Compression Testing

The compression testing was performed with a 22kip MTS load-frame on samples with a $[0]_6$ or $[90]_6$ layup to determine the directional dependent compressive stiffness and strength properties. The crosshead displacement rate was set to 1mm/min, as described by the Modified ASTM D 695 Compression Test. Load vs displacement data was recorded at 10Hz. The DIC system was not used to measure strain since the sample surface was mostly obscured by the fixture. A rectangular sample was placed into the modified Boeing test fixture. Four screws were tightened by hand to secure the sample vertically in place while allowing the sample to freely slide vertically. Vertical alignment of the sample was ensured by firmly pressing the sample against the two alignment pins on the test fixture. The compressive load was introduced through the top of sample with a flat platen. The exposed sample above the test fixture was approximately 3mm. An example of the experimental setup is shown in Figure31. The test was concluded once the sample crushed, buckled, or did not fail, but the platen was too close to the test fixture.

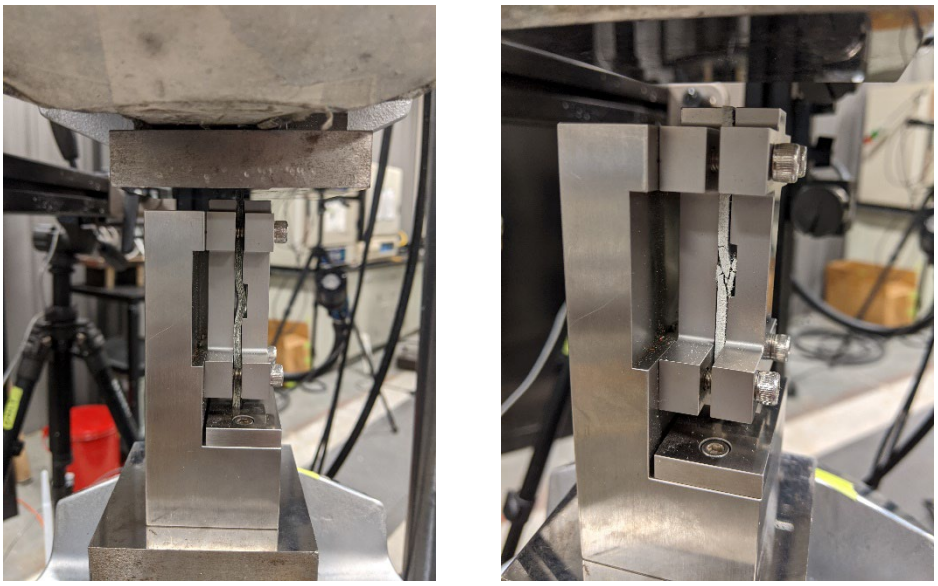

Figure 31: Compression test setup using the standard modified D695 test fixture. Samples are from a failed 0° sample (left) and 90° (right).

The compressive strain (ϵ_c) of the sample was calculated using the following approximation, where sample length is L.

$$\varepsilon_c = \frac{\Delta L}{L} \tag{17}$$

The compressive stress (σ_c) of the sample was calculated using the same equation for tensile stress, force divided by the average cross-sectional area. The strength was defined as the maximum compressive stress experienced by the sample. The compressive modulus (E_c) was calculated as the slope of the linear portion of the stress-strain curve from the test.

$$\sigma_c = \frac{P}{wt} \tag{18}$$

$$E_c = \frac{\Delta\sigma_c}{\Delta\varepsilon_c} \tag{19}$$

Flexure Testing

The compression testing was performed with a 5kip MTS load-frame on samples with a $[0]_6$ or $[90]_6$ layup to determine the directional dependent flexural stiffness and strength properties. The crosshead displacement rate was set to 1mm/min, as described by the ASTM D7264 [5]. Typically, a 32:1 span to thickness ratio is used, however the IACMI 7.3.3 project noted their woven Kevlar® samples were not failing at 32:1 and moved to a smaller ratio of 16 (which is allowed in the standard), where strength values could be measured. The smaller span to thickness ratio was chosen for this work since the composites characterized had a low fiber content and thermoplastic matrix, which were presumed to be quite flexible. The span to thickness ratio for this work was 14.8:1 because of a slight experimental error when initially measuring the span, hence the small deviation from ASTM D7264's optional span to thickness ratio of 16:1. A 3-pt bending fixture with a 33.9 mm span was used, as shown in Figure 32. The

flexure sample lengths were approximately 203 mm, which are well above the recommended 20% longer than span suggested in the standard. The extra length was in anticipation of the sample having a large displacement to failure. The exact sample lengths were not recorded since these were not used in later calculations. The load and displacement measurements were recorded at 10Hz.

Figure 32: Flexure sample test setup using 3-point bending test fixture with a 33.9mm span.

Flexural stress (σ_f) was calculated using the load applied, the span (L), the average width (w), and thickness (t) of the sample. The flexural strength was defined as the maximum stress experienced by the sample during testing.

$$\sigma_f = \frac{3PL}{2wt^2} \tag{20}$$

The flexural stiffness (E_f) can be calculated from the slope of the load-displacement ($\frac{\Delta P}{\Delta \delta}$) curve along with the span, width, and thickness of the sample.

$$E_f = \frac{L^3}{4wt^3}\frac{\Delta P}{\Delta \delta} \tag{21}$$

Rheological Testing

The temperature and strain rate dependence of the VZL-36D resin's dynamic viscosity (η_D) was measured using a Discovery Hybrid Rheometer. 25mm parallel plate geometry with a sample gap between 800 – 1100 µm was used for each sample. Samples weighed approximately 0.7g. The polyamide-6 resin was

pre-dried at 80°C for 14 hours at ambient pressure with no purge gases used. The rheometer chamber was purged with a steady 8LPM of N_2 to help prevent the sample from degrading in air. Resin samples were loaded into a preheated rheology chamber and were melted in between the parallel laminates. The samples were trimmed to prevent any excess material sticking out between the parallel laminates and removed any material on the top plate (since this would influence the inertial calibration).

The samples would dwell at the test temperature for 30 seconds before experiencing a range of strain rates (ω, in radians/sec) ranging in frequencies from 1 to 50Hz with 5 points per decade at a constant strain of 0.03. The strain control mode used with the Trios software was "non-iterative sampling" with an initial stress of 10 µN.m. The tested temperatures ranged from 250 – 290°C in 5°C increments. The dynamic viscosity was defined by the ratio of the loss modulus (G") to the strain rate. The dynamic viscosity was defined by the Cross Model [6] which relates the zero ($\eta_{o,shear}$) and infinite ($\eta_{\infty,shear}$) shear rate viscosities (functions of temperature) with the shear rate (γ, in Hz) dependence of the polymer melt. The zero and infinite shear rate viscosities are defined using the Arrhenius model for viscosity where the activation energy for flow is E_η, R is the ideal gas constant, T is temperature in Kelvin, and η_∞ is the viscosity at a constant shear rate extrapolated to infinite temperature. The Cross Rate Constant (m) and the Cross Time Constant (C) were empirically fitted to the rheological data.

$$\eta_D = \frac{G"}{\omega} \tag{22}$$

$$\eta_i = \eta_\infty e^{\frac{E_\eta}{RT}} \tag{23}$$

$$\eta_D(T) = \eta_{\infty,shear} + \frac{\eta_{0,shear} - \eta_{\infty,shear}}{1 + (C\gamma)^m} \tag{24}$$

Coefficient of Thermal Expansion Testing

The coefficient of thermal expansion (α_i) was determined using the DIC method with a hot stage. Three unidirectional samples were tested to determine the CTE values for the 0° and 90° directions. A 37.5 mm square sample was placed on release film inside a hot stage such that the sample surface could be viewed through the 25mm diameter window. The sample was ramped from room temperature to 140°C at 4°C/min with 8 minute isothermal dwells every 10°C. A single camera was used to record images at 0.2Hz, this data was synced with the temperature recordings of the sample surface. The strain (ϵ_i) measurements were recorded as the average strain during the isothermal dwell once the sample temperature (T) had reached equilibrium. This method was used as this has given more reliable measurements than the dynamic scans without isothermal dwell. The coefficient of thermal expansion was determined by comparing the linear slope of the principal strain vs temperature curve.

$$\alpha_i = \frac{\Delta\epsilon_i}{\Delta T} \tag{25}$$

Results & Discussion

Tensile Samples

Laminates 23 and 26 were used to determine the stiffness and strength in the fiber direction of the Kevlar®/VZL-36D composites. Figure 33 shows the failed tensile samples from laminates 23 and 26. All of the tensile samples from plate 26 failed in the gage section and had a clear fiber failure classified by a lateral failure in the gage section towards one end of the gage section with some long splitting observed in some samples. In plate 23, samples 23_0_T_03 and 23_0_T_04 failed in the grip section, otherwise the samples followed the failure pattern scene in plate 26. Samples 23_0_T_04, 23_0_T_05, and 23_0_T_06 from plate 23 were noted to have some fiber misalignment visible on at the sample surface. This was likely caused during the compression molding of the plate and these samples were not included in the strength or stiffness measurements.

Figure 33: Failed 0° tensile samples from laminates 23 and 26.

Twelve samples were tested from laminates 23 and 26 for 0° mechanical properties. All samples exhibited a linear stress vs strain curve until failure, shown in Figure 34. The 0° samples failed consistently at a strain between 1.6 and 1.8%, with two samples from plate 23 failing before 1.6%. These were a part of the samples that had a disturbance in the fiber orientation during compression molding and can be disregarded. The Young's modulus (E_1) was found to be 27.40 $\pm$ 0.80 GPa and the ultimate tensile strength to be 463.8 $\pm$ 28.4 MPa. While, the strength values were reported, the true strength value was likely higher since a dog-bone geometry was used. These values are reported in Table 16.

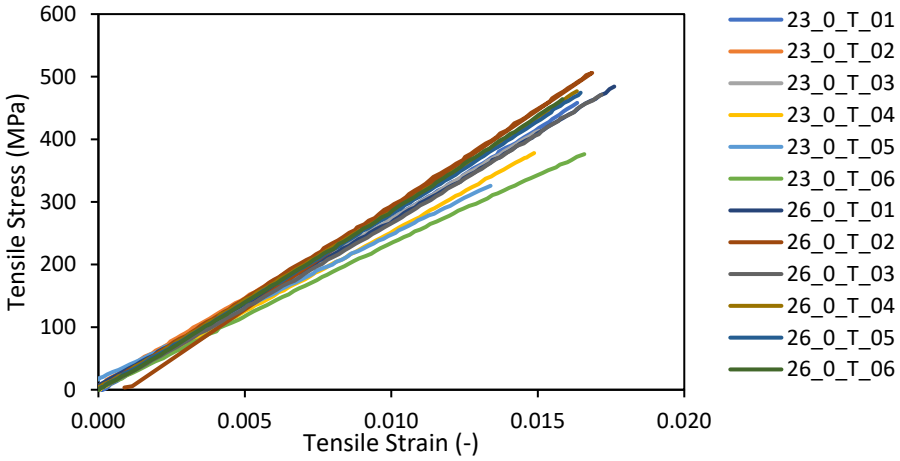

Figure 34: Stress vs strain curve for 0° samples from laminates 23 and 26.

The tensile stiffness values along the fiber direction were low for Kevlar®49 fiber composites at this fiber volume fraction (0.35). . Rules of mixtures would predict the stiffness to be 43 GPa at this fiber volume fraction for Kevlar® 49 fibers, shown in Figure 35. The upper-bound modulus rule of mixtures was used to predict the composite's modulus in the fiber direction. A fiber modulus (E_{fiber}) value of 124 GPa was used to represent the composite with Kevlar® 49 fibers. Because of the large discrepancy, between

experimental and predicted stiffness, a fiber modulus of 83 GPa was used as well to model the composite with Kevlar® 29 fibers. Both curves used the stiffness of the resin (E_{resin}) as 3.58 GPa, because this was the experimentally determined E_2 value which should represent the resin's modulus. The Kevlar® fibers in the composite were confirmed to be Kevlar® 49 fibers.Evaluation of a literature reference (Yeung and Rao) that compared predicted vs. experimental values for three different unidirectional Kevlar®/ thermoplastic resin composites showed similar drop in predicted vs. experimentally determined tensile modulus. Specifically, they found that Rule of Mixtures would have predicted tensile modulus of approximately 93 GPa for the set of composites under study, but, experimental results showed measured values at about 9.3 GPa for the studied systems. It was suggested that iber/resin compatibility at the material interface, or voids, or other fiber packing defects, or microdefects in the structures could be causes. [7] Caminero et. al., found tensile modulus of 3-D printed nylon/Kevlar® 49 composites to be in the range of 27 MPa, and also highlighted the importance of bonding of the polymer to the fiber surface when describing the results [11]. Additionally, while fiber volume fraction was uniform across the width of the tape in this study, evaluation of the micrograph in Figure 27 shows that there was bundling of the filaments within tape, leading to filament-rich and matrix-rich regions. Uniform wetting of the filaments by the matrix is desirable for optimization of product properties, as previously mentioned. Exposure to the Kevlar® fibers to high temperatures during the extrusion process could have contributed as well. No additional experimentation was undertaken to further elucidate the reasons for the lower than predicted modulus in this case, due to time and budget constraints, though this should be considered for future work.

$$E_1 = E_{fiber}\, V_f + E_{resin}(1 - V_f) \tag{26}$$

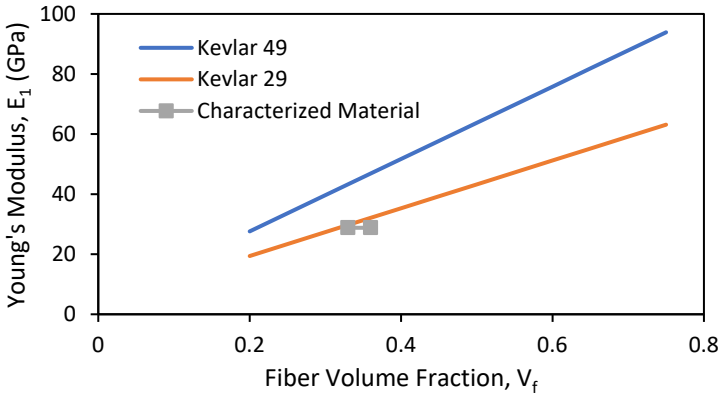

Figure 35: Rules of mixing for tensile Young's modulus in the fiber direction for Kevlar® 29 and 49 fibers compared to the experimentally measured values for Kevlar®/VZL-36D prepreg.

Table 16: Tensile modulus and strength results from laminates 23 and 26 for the 0° samples

Sample Name	Tensile Modulus [GPa]	Tensile Strength [MPa]
23_0_T_01	27.46	459.9
23_0_T_02	28.03	417.1
23_0_T_03	27.34	414.3
~~23_0_T_04~~	~~25.22~~	~~377.6~~
~~23_0_T_05~~	~~22.65~~	~~325.8~~
~~23_0_T_06~~	~~22.90~~	~~375.7~~
26_0_T_01	26.25	484.8
26_0_T_02	28.34	505.6
26_0_T_03	25.90	475.7
26_0_T_04	27.72	476.9
26_0_T_05	27.36	475.1
26_0_T_06	28.29	464.9
Average	27.41	463.8
Std	0.80	28.4

Twelve tensile samples from laminates 24 and 25 were tested to determine the 90° mechanical properties. Samples 23_0_T_04, 23_0_T_05, and _0_T_06 exhibited some fiber shifting at the surface. The samples were still tested, but were omitted from the sample population because of the disturbances to the fiber alignment. The samples had a linear stress vs strain curve until failure, although the data was noisier since the 90° samples did not carry as much load as the 0° samples. The 90° samples all exhibited lateral failure parallel to the fibers and failed inside the gage length. Some samples exhibited failure in multiple locations, but the mode was the same at both locations. The failed samples are shown in Figure 36. The samples all failed at strains from 0.75 – 1.04%, except for sample 24_90_T_01 from plate 24. It was unclear why this sample failed at a lower stress vs strain than all other 90° samples. Since this sample was near the edge of the plate there was a possibility that a defect was introduced during compression molding, which effected this sample, but not the others. Additionally, the stress vs strain curve in Figure 37 show the samples carried a finite load at 0% strain. This was caused by some of the samples being loaded incorrectly and allowing the test to begin while the sample was pre-loaded. This occurred when the hydraulic grips closed on the sample and compressed the sample, then the crosshead was moved to return the sample to a neutral position. Unfortunately, the samples showed low strength values, which meant small changes in the initial loading conditions were evident in the stress vs strain curve. This difference in initial loading did not influence the Young's modulus or strength measurements. The Young's modulus (E_2) was found to be 3.55 $\pm$ 0.52 GPa and the ultimate tensile strength to be 30.8 $\pm$ 2.2 MPa. These values are reported in Table 17.

Figure 36: Failed 90° tensile samples from laminates 24 and 25.

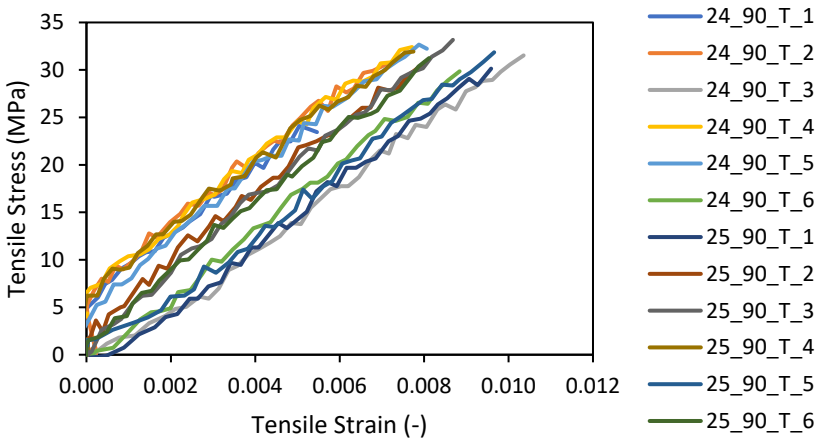

Figure 37: Tensile stress vs strain curve for 90° samples from laminates 24 and 25.

Table 17: Tensile modulus and strength results from laminates 24 and 25 for the 90° samples

Sample Name	Tensile Modulus [GPa]	Tensile Strength [MPa]
24_90_T_1	3.53	24.1
24_90_T_2	3.57	30.7
24_90_T_3	2.26	31.5
24_90_T_4	3.60	32.4
24_90_T_5	3.80	32.0
24_90_T_6	3.52	29.8
25_90_T_1	3.08	30.1
25_90_T_2	4.12	30.8
25_90_T_3	4.00	33.1
25_90_T_4	3.96	31.9
25_90_T_5	3.04	31.8
25_90_T_6	4.09	31.3
Average	3.55	30.8
Std	0.52	2.2

Shear Samples

Five shear samples were tested from laminate 31. In Figure 38, the stress vs strain curves for the shear samples remained linear until ~2% strain where the samples became nonlinear. The samples failed at strains ranging from 8% to 25% with an average ultimate shear stress of 50.1 $\pm$ 4.8 MPa. The shear modulus was calculated from the linear region of the stress vs strain curve, below 2% strain. The shear modulus was found to be 1.12 $\pm$ 0.06 GPa. Shear modulus and strength values for each sample are reported in Table18.

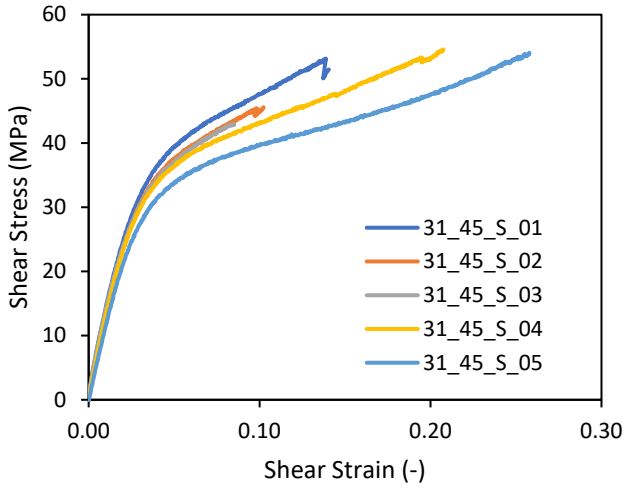

Figure 38: Shear stress vs strain for samples from laminate 31 with layup $[\pm 45]_{2S}$

Table 18: Shear modulus and strength results from laminate 31

Sample Name	Shear Modulus [GPa]	Shear Strength [MPa]
31_45_S_1	1.19	53.2
31_45_S_2	1.14	45.6
31_45_S_3	1.13	43.0
31_45_S_4	1.11	54.6
31_45_S_5	1.01	54.0
Average	1.12	50.1
Std	0.06	4.8

Compression Samples

Ten 0° and ten 90° compression samples were tested to failure or to the strain limit of the test fixtures. The 0° exhibited buckling in the gage section of the test fixture and the 90° samples experienced a shear failure. Figure 40 shows typical examples of the compression samples failing. The samples did not fail at the end, instead, the failure occurred in the gage section. Note, in the case of the samples failing by buckling, the buckling occurred in the small, local region of the fixture where a cut-out was present to allow for a strain gage. All other sections of the specimen were supported on both lateral faces, and hence were constrained from buckling. Some samples did not fail by the time the crosshead platen reached the test fixture; in those cases, the ultimate stress was recorded at the maximum stress the samples carried before the crosshead reached the test fixture.

The 0° compression samples stress vs strain curves in Figure 39 showed a linear stress vs strain region with strains ranging from 0.2% to 0.8%. The Young's modulus was calculated from this linear region. The stress vs strain curve below 0.2% was nonlinear, which was caused by the sample settling slightly in the test fixture. All 0° samples exhibited non-linearity beyond 1% strain. The 0° samples exhibited consistent stress vs strain curves, except for sample 23_0_C_01. This was the first sample tested and the screws holding the sample in place may have been too loose. This did not impact the modulus or strength values significantly. The 0° compressive Young's modulus was 10.47 $\pm$ 1.39 GPa and the compressive strength was 131.5 $\pm$ 6.5 MPa with results for each sample reported in Table 19. The compressive properties in the fiber direction are significantly worse than in tension. This result was expected as Kevlar® has poor compressive stiffness and strength.

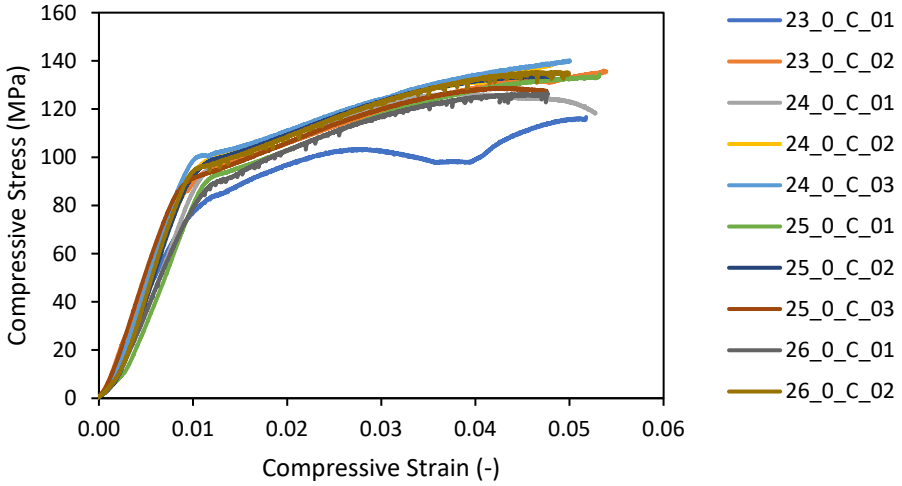

Figure 39: Compressive stress vs strain curves for unidirectional 0° samples.

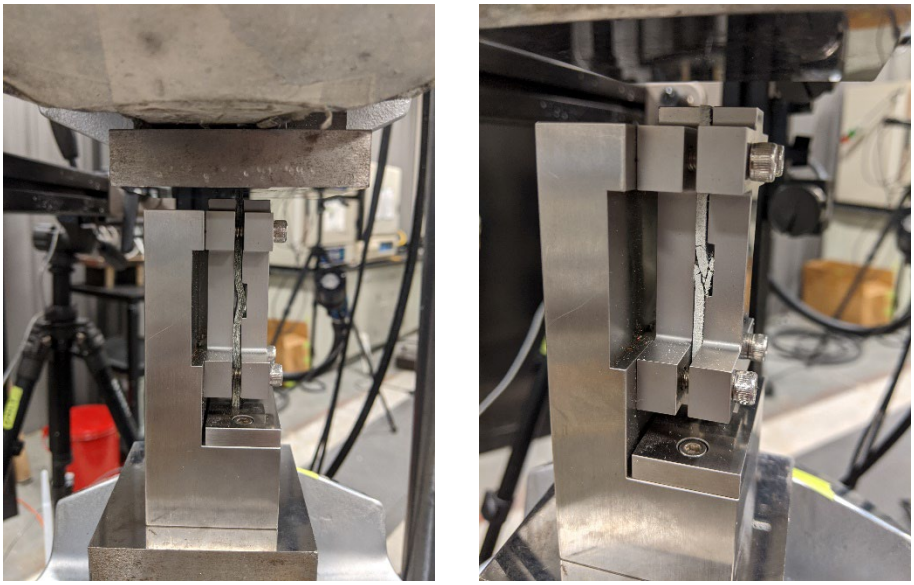

Figure 40: Typical failure examples for compression 0° samples (left) in buckling and 90° samples (right) in shear.

Table 19: Compression modulus and strength results from laminates 23, 24, 25, and 26 for the 0° samples.

Sample Name	Compressive Modulus [GPa]	Compressive Strength [MPa]
23_0_C_1	9.48	116.7
23_0_C_2	9.90	136.0
24_0_C_1	8.83	126.5
24_0_C_2	10.65	138.4
24_0_C_3	12.19	138.3
25_0_C_1	8.39	134.4
25_0_C_2	11.40	134.0
25_0_C_3	11.72	128.8
26_0_C_1	9.47	126.5
26_0_C_2	12.62	135.4
Average	10.47	131.5
Std	1.39	6.5

The 90° compression samples stress vs strain curves in Figure 41 shows a linear stress vs strain region with strains ranging from 0.8% to 2%. The Young's modulus was calculated from this linear region. The stress vs strain curve below 0.8% was nonlinear, which was caused by the sample settling slightly in the test fixture. All 90° samples exhibited non-linearity beyond 2.2% strain. The 90° samples exhibited slightly less consistent stress vs strain curves compared to the 0° samples. This was probably caused by the lower loads and sample settling into the fixture. The 90° compressive Young's modulus was 13.13 $\pm$ 0.30 GPa and the compressive strength was 89.7 $\pm$ 8.0 MPa with results for each sample reported in Table 20. The compressive Young's modulus in the transverse fiber direction are very similar to the tensile modulus which was expected. The ultimate compressive strength was significantly larger than the tensile

strength suggesting the resin did not form a strong bond with the fibers. This poor resin/fiber interaction contributed to premature failure in the tensile coupons.

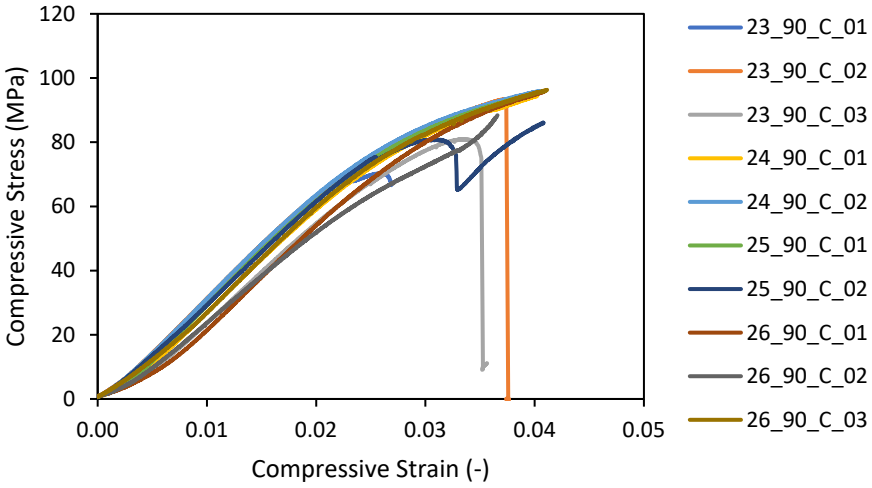

Figure 41: Compressive stress vs strain curves for unidirectional 90° samples.

Table 20: Compression modulus and strength results from laminates 23, 24, 25, and 26 for the 90° samples.

Sample Name	Compressive Modulus [GPa]	Compressive Strength [MPa]
23_90_C_1	3.32	70.7
23_90_C_2	3.38	93.3
23_90_C_3	3.14	80.9
24_90_C_1	3.30	94.5
24_90_C_2	3.39	95.9
25_90_C_1	3.35	95.0
25_90_C_2	3.26	86.1
26_90_C_1	2.50	95.8
26_90_C_2	2.68	88.4
26_90_C_3	3.02	96.3
Average	3.13	89.7
Std	0.30	8.0

Flexure Samples

Nine 0° flexure samples from laminates 23 and 26 were tested in 3-point bending with the resulting load vs displacement curves shown in Figure 42. Sample 23_0_F_01 was tested with an incorrect span and was not reported. The span used for the remaining nine samples was 33.9mm to give a span to thickness ratio of 14.7. The narrower span was chosen because of the flexibility noted by the IACMI 7.3.3 project. The load vs displacement curve was linear until a displacement of 0.4mm. The Young's modulus was calculated from this linear region. All 0° flexure samples exhibited nonlinearity above 0.6mm. The 0° flexural Young's modulus was 21.34 $\pm$ 0.69 GPa and the flexural strength was 345.5 $\pm$ 39.2 MPa with results for each sample reported in Table 21.

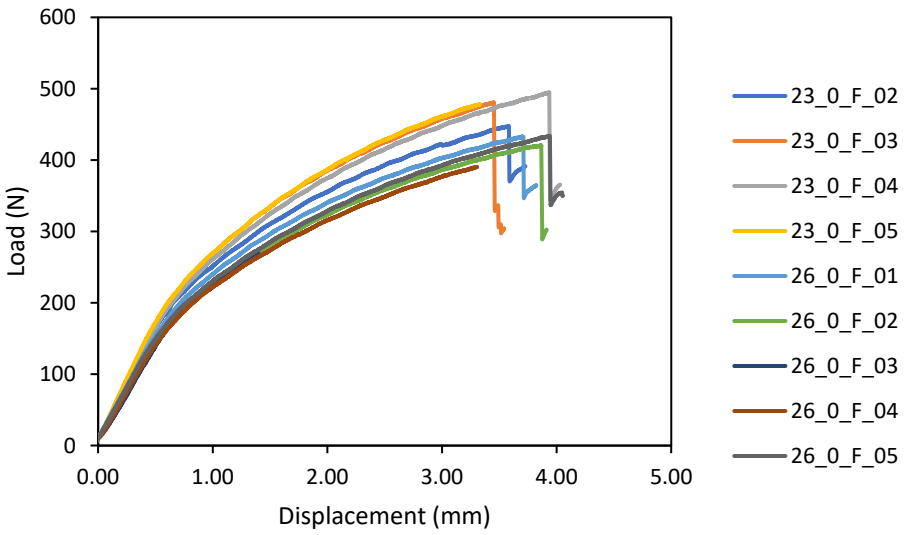

Figure 42: 3-point bending load vs displacement curve for 0° samples from laminates 23 and 26.

Table 21: Flexural modulus and strength results from laminates 23 and 26 for the 0° samples.

Sample Name	Flexural Modulus [GPa]	Flexural Strength [MPa]
23_0_F_02	21.80	356.3
23_0_F_03	22.90	362.0
23_0_F_04	21.44	380.7
23_0_F_05	20.44	351.7
26_0_F_01	21.35	365.8
26_0_F_02	20.86	354.8
26_0_F_03	21.08	239.1
26_0_F_04	20.67	337.2
26_0_F_05	21.56	361.7
Average	21.34	345.5
Std	0.69	39.2

Ten 90° flexure samples from laminates 24 and 25 were tested in 3-point bending with the resulting load vs displacement curves shown in Figure 43. Sample 23_0_F_01 was tested with an incorrect span and was not reported. The span used was 33.9mm to give a span to thickness ratio of 14.7. The narrower span was chosen because of the flexibility noted by the IACMI 7.3.3 project. The load vs displacement curve was linear until 0.6mm of displacement. The Young's modulus was calculated from this linear region. The 90° flexural Young's modulus was 3.58 $\pm$ 0.42 GPa and the flexural strength was 45.8 $\pm$ 4.0 MPa with results for each sample reported in Table 22.

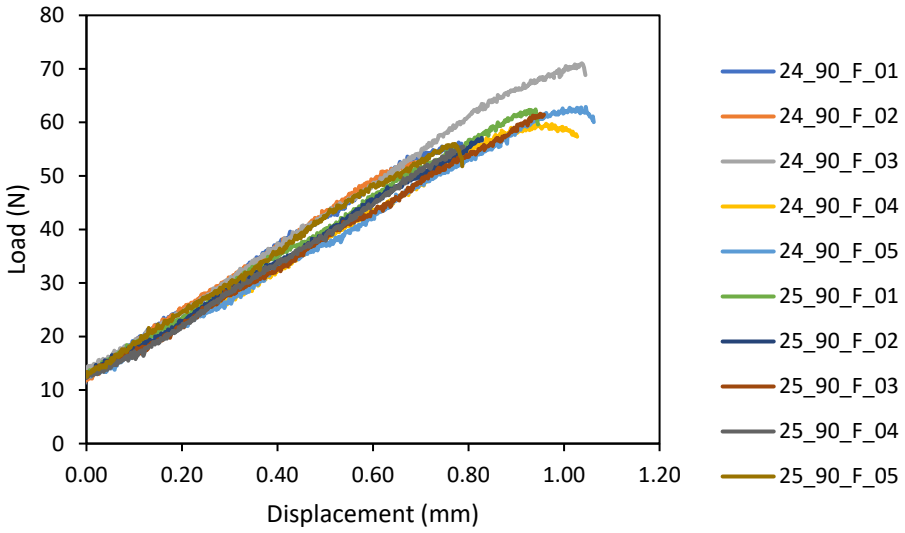

Figure 43: 3-point bending load vs displacement curve for 90° samples from laminates 24 and 25.

Table 22: Flexural modulus and strength results from laminates 24 and 25 for the 90° samples.

Sample Name	Flexural Modulus [GPa]	Flexural Strength [MPa]
24_90_F_01	3.75	43.2
24_90_F_02	3.78	39.8
24_90_F_03	3.51	51.9
24_90_F_04	2.96	42.6
24_90_F_05	2.67	41.6
25_90_F_01	3.51	49.0
25_90_F_02	3.83	47.1
25_90_F_03	3.80	51.7
25_90_F_04	4.07	46.6
25_90_F_05	3.88	44.1
Average	3.58	45.8
Std	0.42	4.0

Rheological Characterization

The neat VZL-36D resin was subjected to oscillatory shear with frequencies ranging from 1 – 50 Hz. The resin exhibited shear thinning behavior across these frequencies. The temperature and frequency dependence of the resin is shown in Figure 44. In these tests, the resin was able to achieve a low melt viscosity, 15 Pa•s, which makes this resin well suited for prepreg manufacturing. However, the resin surface was noted to become unstable above 300°C, as such tests above 290°C were not included. The sample surface would oxidize with the air in the chamber, despite the sample chamber receiving a steady nitrogen flow. Even with nitrogen flow, the chamber was not airtight, which allowed the oxidation to occur. The sample would only show signs of degradation at the surface in the form of a "skin" layer forming. This skin layer would influence the viscosity measurements and cause a slightly elevated viscosity measurement for that temperature. This was not considered to be an issue during prepregging since the resin would not be in contact with air while in the die at elevated temperatures. Additionally, these effects were only noted when the sample would remain above 290°C for 10 minutes.

The viscosity data for the VZL-36D resin was fitted to the Cross Model as this has been shown to describe shear thinning polymers. The Cross Rate Constant (m) was found to be 0.52 and the Cross Time Constant (C) was found to be 0.93 seconds. The zero and infinite shear Arrhenius fitting parameters are shown in Table 23. These fitting parameters provided a good fit for the data shown in Figure 44.

Table 23: Arrhenius parameters for the zero and infinite shear viscosities of the VZL-36D resin.

	E_η [kJ/mol]	η_∞ [Pa•s]
Zero shear ($\eta_{0,shear}$)	50.75	3.26E-04
Infinite shear ($\eta_{\infty,shear}$)	54.85	3.17E-04

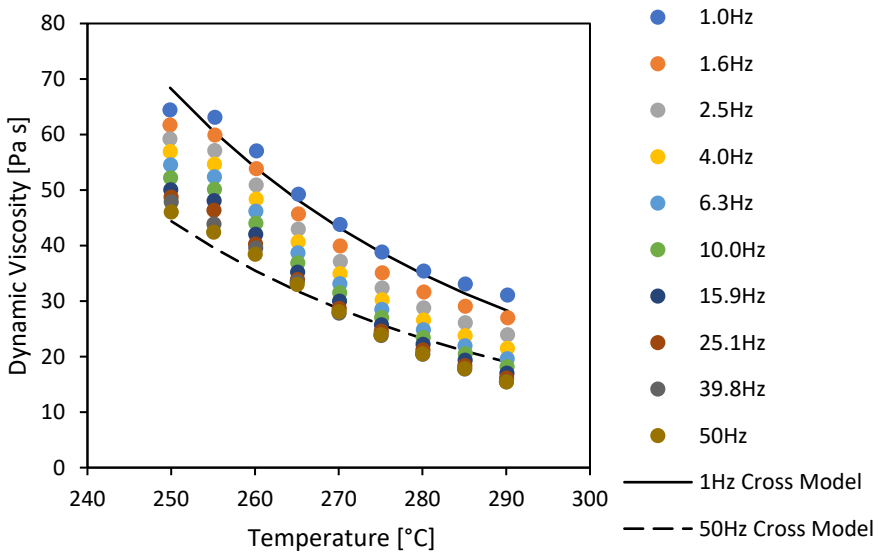

Figure 44: VZL-36D resin dynamic viscosity vs frequency for temperatures 250 to 290°C. For clarity, the Cross Model fit is shown for 1Hz and 50Hz, demonstrating the model fit.

Thermoelastic Characterization

Three coefficient of thermal expansion samples were tested from laminates 24, 25, and 26. The same sample and test was able to measure the thermal strains in the 0° and 90° directions. Plate 23's sample was broken when cutting out the sample and was not tested. The thermal strain vs temperature curves are shown in Figure 45. The thermal strains in the fiber direction (0°) were nearly zero with a CTE_1 of -2.0 $\pm$ 1.9 µ/°C, which was expected for Kevlar® fiber composites. The thermal strains transverse to the fiber direction (90°) were significantly larger. The CTE_2 below the T_g (80°C) was 171.2 $\pm$ 3.2 µ/°C and above the T_g (100°C) was 189.3 $\pm$ 6.2 µ/°C. These CTE_1 and CTE_2 values for each sample were reported in Table 24 and Table 25, respectively. The sample from plate 24 exhibited strange behavior above the T_g. An error likely occurred during testing, however the precise reason for this discrepancy was unclear, as a result this sample was omitted when reporting the CTE values.

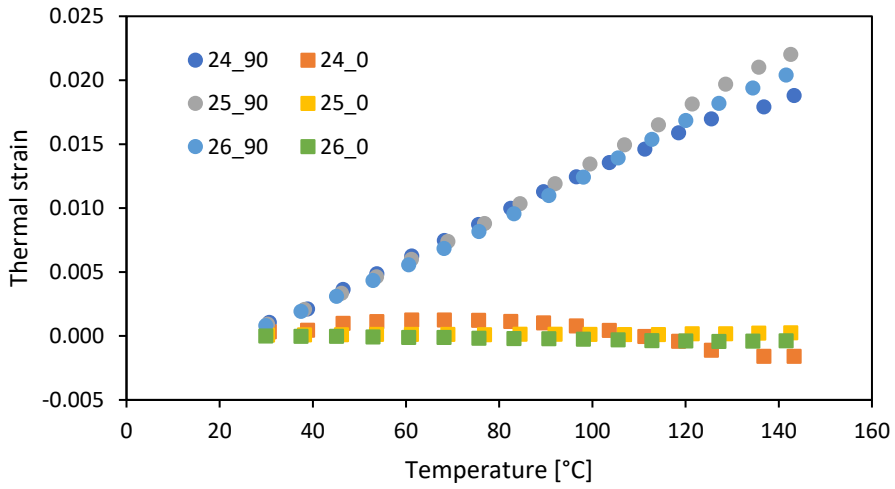

Figure 45: Thermal strain vs temperature curves from laminates 24, 25, and 26 for strains in the 0° and 90° directions

Table 24: Coefficient of thermal expansion along the fiber direction for samples from laminates 24, 25, and 26.

Sample Name	CTE_1 below Tg [µ/°C]	CTE_1 above Tg [µ/°C]
~~24_0~~	~~1.4~~	~~-46.1~~
25_0	-0.1	3.8
26_0	-3.9	-0.8
Average	-2.0 ± 1.9	1.5 ± 2.3

Table 25: Coefficient of thermal expansion transverse to the fiber direction for samples from laminates 24, 25, and 26.

Sample Name	CTE_2 below Tg [µ/°C]	CTE_2 above Tg [µ/°C]
~~24_90~~	~~175.1~~	~~125.0~~
25_90	174.4	195.5
26_90	168.0	183.1
Average	171.2 ± 3.2	189.3 ± 6.2

Conclusions

This report covered the hot melt manufacturing process used at the Manufacturing Design Laboratory to produce Kevlar®/polyamide-6 prepreg tape. The VZL-36D resin (polyamide-6) was characterized for its rheological properties and was found to exhibit shear thinning. The Cross Model provided an excellent fit of the rheological data. Additionally, the prepreg tape was studied to experimentally determine the directionally dependent: tensile, compression, flexure, shearing, and thermoelastic properties of Kevlar® 49/VZL-36D prepreg. The mechanical properties for the prepreg tape with a fiber volume fraction of 0.35 is summarized in Table 26. The 0° tensile stiffness was lower than expected for Kevlar® 49 fibers. Additionally, the 90° tensile strength was very low compared to the compressive strength in the same direction. This suggests the resin/fiber interface was poorly bonded. This clearly deserves further investigation, including possibly of sizing and other processing effects. See the Commercialization section at the end of the report for more discussion. However, as an initial proof-of-concept, the project

was deemed successful for prototyping a unidirectional Kevlar® prepreg and characterizing its properties. The mechanical properties reported are common inputs required for material models in most finite element simulation software for performance simulations. Further evaluation of these material systems may allow broader incorporation of these materials into modeling and simulation of software packages.

Table 26: Summary of material properties from characterization tests for Kevlar®/VZL-36D prepreg.

Sample Type	Modulus (GPa)	Strength (MPa)	ν_{12}
Tension [0°]	27.41 ± 0.80	463.8 ± 28.4	0.45 ± 0.05
Tension [90°]	3.55 ± 0.52	30.8 ± 2.2	
Compression [0°]	10.47 ± 1.39	131.5 ± 6.5	
Compression [90°]	3.13 ± 0.30	89.7 ± 8.0	
Flexure [0°]	21.3 ± 0.7	345.5 ± 39.2	
Flexure [90°]	3.58 ± 0.42	45.8 ± 4.0	
Shear	1.12 ± 0.06	50.1 ± 4.8	

Appendix A1: Prepreg and Laminate Process Conditions

Table 27: Compression molding conditions for Kevlar®/VZL-36D prepreg

Plate #	Prepreg ID	Layup	Press Force [ton]	Peak Press Temperature [C]
1	0	$[0]_4$	5	254
2	0	$[0]_8$	5	276
3	0	$[(0/90)_2]_S$	5	277
4	12041	$[0]_8$	5	273
5	12051	$[0]_8$	5	271
6	6	$[0]_8$	5	267
7	10	$[0]_8$	5	266
8	12	$[0]_8$	5	269
9	12041	$[0]_8$	5	259
10	14	$[0]_8$	5	269
11	15	$[0]_8$	3	270
12	16	$[0]_3$	3	265
13	18	$[0]_8$	3	265
14	17	$[(0/90)_4]$	3	267
15	17	$[90/0_3]_S$	3	268
16	20	$[90/0_3]_S$	3	265
17	15	$[90/0_3]_S$	3	262
18	15	$[90/0_3]_S$	3	282
19	24	$[0]_8$	3	264
20	28.2	$[0]_6$	3	253
21	28.2	$[0]_6$	3	245
22	28.2	$[0]_6$	3	253
23	28.2	$[0]_6$	3	246
24	28.2	$[0]_6$	3	250
25	28.2	$[0]_6$	3	250
26	28.2	$[0]_6$	3	248
27	29.1	$[0]_6$	3	248
28	30.1	$[0]_6$	3	250
29	30.1	$[0]_6$	3	251
30	28.2	$[0,90]_{2S}$	3	250
31	28.2	$[0,90]_{2S}$	3	248

Table 28: Prepreg manufacturing conditions for Kevlar®/VZL-36D thermoplastic unidirectional tape

Name	Pump Speed [RPM]	Line Speed [FPM]	Yarn Count	Die Temp [°C]	Expected V_f
1	42.0	5.0	36	310	
2	36.0	5.0	36	310	
3	30.0	5.0	36	310	
4	36.0	5.0	36	310	
5	36.0	5.0	36	310	
6	34.0	5.0	36	310	
7	58.0	8.0	36	310	
8	58.0	7.8	36	310	
9	58.0	7.5	36	310	
10	34.0	5.0	35	310	
11	14.4	2.0	32	310	
12	16.5	2.0	32	310	
13	15.5	2.0	32	310	
14	14.8	2.0	32	310	
15	14.5	2.0	32	310	
16	14.4	2.0	28	310	
17	14.4	2.0	24	310	
18	14.5	2.0	26	310	0.51
19	14.5	2.0	26	310	0.51
20	13.5	2.0	26	310	0.52
21	14.5	2.0	26	290	0.51
22	19.0	2.0	26	310	0.43
23	30.0	2.0	26	310	0.33
24	30.0	2.0	26	310	0.33
25	30.0	2.0	26	310	0.33
26	60.0	4.0	26	310	0.33
27	42.0	3.0	26	310	0.34
28	40.0	3.0	26	310	0.35
29	15.0	1.5	26	310	0.42
30	45.0	4.5	26	310	0.42
31	12.0	2.0	26	310	0.55

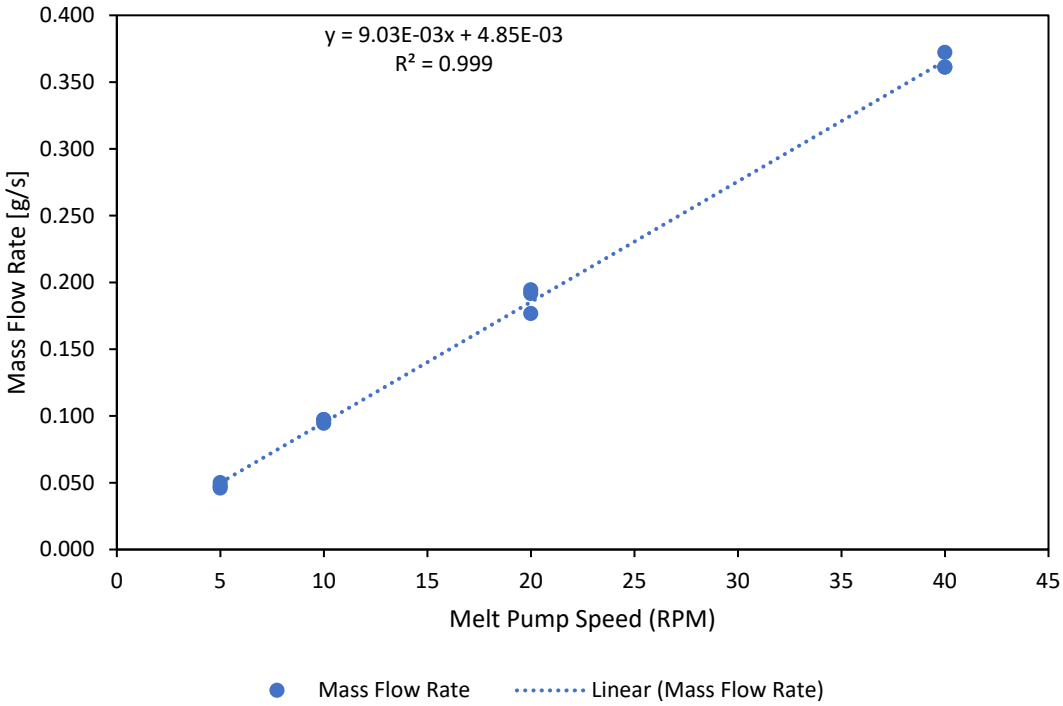

Figure 46: Prepreg line melt pump calibration curve with VZL-36D resin at 260°C.

Appendix A2: Mechanical Testing Sample Dimensions

Table 29: 0° tensile sample dimensions from the Kevlar®/VZL-36D prepreg

Sample Name	Width [mm]	Average [mm]	Thickness [mm]	Average [mm]
23_0_T_1	12.65	12.62	2.41	2.40
23_0_T_2	12.61		2.45	
23_0_T_3	12.65		2.39	
23_0_T_4	12.64		2.39	
23_0_T_5	12.65		2.39	
23_0_T_6	12.49		2.39	
26_0_T_1	12.53	12.52	2.44	2.36
26_0_T_2	12.55		2.41	
26_0_T_3	12.53		2.36	
26_0_T_4	12.54		2.35	
26_0_T_5	12.51		2.31	
26_0_T_6	12.46		2.31	

Table 30: 90° tensile sample dimensions from the Kevlar®/VZL-36D prepreg

Sample Name	Width [mm]	Average [mm]	Thickness [mm]	Average [mm]
24_90_T_1	12.89	12.86	2.22	2.25
24_90_T_2	12.86		2.22	
24_90_T_3	12.89		2.23	
24_90_T_4	12.91		2.24	
24_90_T_5	12.85		2.29	
24_90_T_6	12.78		2.27	
25_90_T_1	12.66	12.61	2.27	2.25
25_90_T_2	12.56		2.31	
25_90_T_3	12.56		2.22	
25_90_T_4	12.57		2.25	
25_90_T_5	12.67		2.23	
25_90_T_6	12.62		2.22	

Table 31: ±45° shear sample dimensions from the Kevlar®/VZL-36D prepreg

Sample Name	Width [mm]	Average [mm]	Thickness [mm]	Average [mm]
31_45_S_1	25.33	25.38	3.19	3.16
31_45_S_2	25.39		3.25	
31_45_S_3	25.39		3.29	
31_45_S_4	25.36		3.10	
31_45_S_5	25.41		2.99	

Table 32: 0° compression sample dimensions from the Kevlar®/VZL-36D prepreg

Sample Name	Width [mm]	Average [mm]	Thickness [mm]	Average [mm]
23_0_C_1	12.64	12.64	2.47	2.36
23_0_C_2	12.64		2.26	
24_0_C_1	12.67	12.68	2.21	2.21
24_0_C_2	12.69		2.21	
24_0_C_3	12.68		2.20	
25_0_C_1	12.52	12.49	2.58	2.55
25_0_C_2	12.48		2.56	
25_0_C_3	12.47		2.51	
26_0_C_1	12.55	12.54	2.34	2.26
26_0_C_2	12.53		2.18	

Table 33: 90° compression sample dimensions from the Kevlar®/VZL-36D prepreg

Sample Name	Width [mm]	Average [mm]	Thickness [mm]	Average [mm]
23_90_C_1	12.90	12.90	2.14	2.17
23_90_C_2	12.89		2.16	
23_90_C_3	12.89		2.20	
24_90_C_1	12.87	12.87	2.34	2.33
24_90_C_2	12.88		2.32	
25_90_C_1	12.67	12.67	2.14	2.23
25_90_C_2	12.66		2.33	
26_90_C_1	12.70	12.72	2.19	2.17
26_90_C_2	12.74		2.18	
26_90_C_3	12.71		2.14	

Table 34: 0 ° 3-point bending sample dimensions from the Kevlar®/VZL-36D prepreg

Sample Name	Width [mm]	Average [mm]	Thickness [mm]	Average [mm]
23_0_F_1	12.10		2.30	
23_0_F_2	12.08		2.30	
23_0_F_3	12.05	12.19	2.27	2.30
23_0_F_4	12.08		2.31	
23_0_F_5	12.63		2.34	
26_0_F_1	11.95		2.24	
26_0_F_2	11.93		2.22	
26_0_F_3	11.99	12.05	2.19	2.21
26_0_F_4	11.95		2.22	
26_0_F_5	12.44		2.19	

Table 35: 90° 3-point bending sample dimensions from the Kevlar®/VZL-36D prepreg

Sample Name	Width [mm]	Average [mm]	Thickness [mm]	Average [mm]
24_90_F_1	12.31		2.32	
24_90_F_2	12.28		2.34	
24_90_F_3	12.28	12.39	2.38	2.38
24_90_F_4	12.27		2.41	
24_90_F_5	12.82		2.45	
25_90_F_1	12.04		2.32	
25_90_F_2	12.07		2.26	
25_90_F_3	12.07	12.17	2.24	2.26
25_90_F_4	12.07		2.24	
25_90_F_5	12.63		2.26	

Appendix A3: Digital Image Correlation Operating Procedure

Basic Equipment and Safety Information

Manufacturer:	Correlated Solutions, Inc.
User Manual and Documentation Location:	[DataDepot]:\CMSC\Lab_Resources\Characterization Lab\DIC - Digital Image Correlation – and – shelf on computer cart
Required Equipment:	DIC Laptop, camera(s), tripod, lighting, DAQ, paint or ink, calibration reference object
Required Software:	VIC-SNAP, VIC-3D, VIC-2D
Potential Safety Hazards:	Speckling involves paint or ink, handle other equipment with care
Required PPE:	safety glasses, gloves when speckling
Point of Contact:	Ben Denos

Purpose and Procedure

Purpose:

The DIC system allows non-contact capture of full field surface strain data in 2D (one camera) or 3D (two cameras). Images are captured using 5MP cameras and VIC-SNAP software. Images are analyzed using VIC-2D/3D software. A stochastic speckle pattern must be applied to specimens.

Procedure:

Preparation

A stochastic speckle pattern must be present or applied on the surface of test specimens. See the Speckle Application Guidelines manual to determine the best process and pattern size for your application. Paint or ink must be pliable enough to deform without stiffening the specimen or separating from its surface. If using spray paint, apply a base coat of white primer and then black speckle by barely holding down the paint can trigger. Use of ink based roller stamps is encouraged for any simple or relatively flat surfaces to ensure consistent pattern coverage.

Power Up

1. Connect cameras to USB 3.0 (blue) ports on laptop, ensure USB license is plugged in
2. Connect NI DAQ box if external data is desired
3. Open VIC-SNAP software and choose the folder where all images will be saved
4. If lights on back of cameras are red, unplug them, close VIC-SNAP, plug them back in, and wait for the “drivers loaded” dialog box to appear. Lights should be green. Resume work.

Calibration – Perform with every new setup

1. Place a specimen in test fixture to use for focusing cameras
2. Check analog data if desired (plugged in?, scaled properly?) -click button with colored line graph
3. Move camera setup and change lenses to get object to fill frames
4. Open apertures to let in most light and narrow depth of field, black ring, finger set screw
5. Loosen focus lock ring set screw, adjust focus, check with zooming and sigma visual (right click)
6. Lock focus set screw on silver ring at base of lens, close aperture to mid level
7. Adjust lighting (physical) and exposure time (in software) to remove overexposure seen as red

8. Choose a calibration object from the case in the black cabinet to fill ¾+ of camera view
9. Click calibration images button and capture calibration images – rotate object about X, Y, Z axes close enough to desired specimen location to remain in focus
10. To verify usable calibration images, click VIC-3D button, click calibrate (caliper icon). If number is green, save calibration project file for use with all analyses in test series
11. DO NOT MOVE OR ADJUST CAMERAS, FOCUS, TRIPOD, OR POSITION ONCE CALIBRATION IS DONE. Only change software parameters and lighting.

Operation

1. Load specimen into test fixture
2. Click speckle images button, click manual capture or choose timed capture options
3. Capture pre-load images if desired
4. Start capture before test begins to get a few reference frames, stop when finished
5. Any DAQ-read data will be captured at the same rate as images

Results

1. Click VIC-3D button to open post processing
2. Open speckle Images from folder if not transferred automatically
3. Select calibration file (Calibration/From Project File/ Select) or calibrate now
4. Draw area of interest (AOI) with tools on left
5. Press the "?" to check recommended subset size. Can go slightly smaller, 31 common
6. Click green "play arrow" icon to run analysis
7. Click the "ϵ" button to calculate strain, filter size is like strain gauge size
8. Right click on data results window to change variable, 2D/3D view, and export video

Power Down

1. Save project files – original images already saved, can always start from them
2. Move data to personal storage device and remove files from laptop
3. Log off and close or power down the laptop, put lens caps back on cameras and turn off lights

Maintenance and Consumables

1. Clean everything off with compressed air and lens cloth if dirty
2. Clean speckle stamp rollers with stamp cleaner
3. Replace speckling ink or paint

1. BENEFITS ASSESSMENT

In an effort to increase fuel economy and safety standard of light-weight vehicles, the automotive industry has been using increasing amounts of composite materials in manufacturing. Kevlar® fiber-containing composite materials have underlying benefits for the automotive industry, like ductile failure mechanisms and impact tolerance, that have not been fully utilized. If material properties of Kevlar® composites more applicable to automotive end-uses are determined, they can be evaluated for addition to widely used manufacturing and performance simulation software packages, to potentially allow for broader adoption of these solutions. This project initiated data collection to that end.

2. COMMERCIALIZATION & RECOMMENDATIONS

This project involved initial data collection on the material properties of two different Kevlar® fiber composite structures, to determine possibility of inclusion of these data into available software modelling systems, with the ultimate goal of allowing for wider use of Kevlar® composites into automotive end-uses.. This initial data collection was successfully completed on both of the planned composite model systems. Conclusions related to the testing of these materials are included in the body of the report.

Additional work, however, would be required for further inclusion of these results into commercial modelling software.
For the woven Kevlar® prepreg from part 7.3.3, additional data would be needed to more broadly incorporate manufacturing and lot-to-lot variability of the raw materials, prior to evaluation for further adoption into software systems. Comparison to other commercially available fiber/resin composites would then be required, to help assess commercial viability of any future work. Future work may consider testing of additional samples for more robust data sets.

More optimization on the properties of the thermoplastic tapes evaluated in project 7.3.4 is likely required before additional commercial consideration of that system can be made. Such work could consider the impact and optimization of the surface properties between the fiber and matrix, as well as uniformity of the resin/matrix structure. Additional investigation of wetting of Kevlar® fiber by epoxy and by polyamide may help further describe measured differences between the two sets of composites measured in this report.

At the time of report issuance, no additional work is planned, and data collected is communicated via release of the project report.

3. ACCOMPLISHMENTS

The planned portions of the project laid out in the research proposal were completed (See note on polymer rheology on page 25), and the results are documented in this report. The expected deliverables from this project were initial data sets that could be evaluated for potential inclusion into modelling systems, to potentially allow for broader adoption of Kevlar® fiber containing composites into automotive applications. Tables of results are included in the technical sections above (p. 1 and p. 26).

Alex Reichanadter's dissertation will focus heavily on work funded by this project.

4. REFERENCES AND/OR BIBLIOGRAPHY

[1] VIC Speckle Kit User Manual. Correlated Solutions; n.d.

[2] Easy Guide Setup Procedures for the VIC-3D 5MP Quasi-Static System. Correlated Solutions; 2013.

[3] ASTM D3039/D3039M-17. Standard Test Method for Tensile Properties of Polymer Matrix Composite Materials. Annu B ASTM Stand 2014:1–13. https://doi.org/10.1520/D3039.

[4] D 3518. Standard Test Method for In-Plane Shear Response of Polymer Matrix Composite Materials by Tensile Test of a 645 ° Laminate 1. Annu B ASTM Stand 2007;94:1–7. https://doi.org/10.1520/D3518.

[5] ASTM D7264/D7264M-07. Standard Test Method for Flexural Properties of Polymer Matrix Composite Materials. Annu B ASTM Stand 2007;i:1–11. https://doi.org/10.1520/D7264.

[6] Xie J, Jin YC. Parameter determination for the cross rheology equation and its application to modeling non-Newtonian flows using the WC-MPS method. Eng Appl Comput Fluid Mech 2016;10:111–29. https://doi.org/10.1080/19942060.2015.1104267.

[7] For dicussion on difference of predicted properties of Kevlar® 49 thermoplastic composites vs. measured properties in alternate thermoplastic resin systems, see for instance Yeung, K. K. H., Rao, K. P. Mechanical Properties of Kevlar-49 Fibre Reinforce Thermoplastic Composites. Polymers and Polymer Composites, 2012; 20: 411-424, and references cited therein.

[8] Carlsson, Adams, and Pipes, "Experimental Characterization of Advanced Composite Materials" Third Edition, 2002.

[9] Fouad, H.; Mourad, A-H., Alshammari, B., Hassan, M. Abdallah, M., Hashem, M.; J. Mech. Behavior Biomedical Materials, 101 (2020) 103456.

[10] Singh, T. J.; Samanta, S. Materials Today: Proceedings, 2 (2015) 1381-1387.

[11] Caminero, M. A., Chacon, J. M.; Garcia-Moreno, I.; Reverte, J. M. Polymer Testing, 68 (2018) 415-423.

5. APPENDICES

See appendices at the end of each technical section.